The Cu(II) reductase RclA protects *Escherichia coli* against the combination of hypochlorous acid and intracellular copper.

Rhea M. Derke[1], Alexander J. Barron[2], Caitlin E. Billiot[1], Ivis F. Chaple[3], Suzanne E. Lapi[3], Nichole A. Broderick[2,4], and Michael J. Gray[1*]

[1] Department of Microbiology, School of Medicine, University of Alabama at Birmingham, 845 19th Street South, Birmingham, AL 35294

[2] Department of Molecular and Cell Biology, University of Connecticut, Storrs, CT 06269 U.S.A.

[3] Department of Radiology, School of Medicine, University of Alabama at Birmingham, 1824 6th Ave South, Birmingham, AL 35233

[4]Institute for Systems Genomics, University of Connecticut, Storrs, CT 06296 U.S.A.

*** Corresponding Author**

Michael J. Gray

656 Bevill Biomedical Research Building

845 19th Street South

Birmingham, AL 35294

205-934-6293

mjgray@uab.edu

ORCID iD: 0000-0002-7112-4188

Subject Area: Microbiology and Infectious Disease

ABSTRACT

Inflammatory bowel diseases (IBDs) are a growing health concern. Enterobacteria, including *Escherichia coli*, bloom to high levels in the gut during inflammation and strongly contribute to the pathology of IBDs. To survive in the inflamed gut, *E. coli* must tolerate high levels of antimicrobial compounds produced by the immune system, including toxic metals like copper and reactive chlorine oxidants like hypochlorous acid (HOCl). In this work, we show that the widely-conserved bacterial HOCl resistance enzyme RclA catalyzes the reduction of copper (II) to copper (I), and specifically protects *E. coli* against the combination of HOCl and intracellular copper, probably by preventing Cu(III) accumulation. *E. coli* lacking RclA were highly sensitive to HOCl and were defective in colonizing an animal host. Our results indicate unexpected complexity in the interactions between antimicrobial toxins produced by innate immune cells and suggest an important and previously unsuspected role for copper redox reactions during inflammation.

INTRODUCTION

Inflammatory bowel diseases (IBDs), like Crohn's disease and ulcerative colitis, are a growing health problem (1), and are associated with dramatic changes in the composition of the gut microbiome (2-6). Patients with IBDs have increased proportions of proteobacteria, especially *Escherichia coli* and other *Enterobacteriaceae*, in their gut microbiomes, which is thought to contribute to the progression of disease (7-10). The bloom of enterobacteria in the inflamed gut is driven by increased availability of respiratory terminal electron acceptors (*e.g.* oxygen, nitrate, TMAO) and carbon sources (*e.g.* ethanolamine, mucin), which *E. coli* and other facultative anaerobes can use to

48 outcompete the obligate anaerobes (*Bacteroides* and *Clostridia*) that dominate a healthy
49 gut microbiome (2, 3). In addition to these nutritional changes in the gut environment,
50 inflammation also leads to infiltration of innate immune cells (*e.g.* neutrophils) into the
51 lumen of the gut (11) and an associated increased production of antimicrobial
52 compounds by the innate immune system (9, 10, 12), which also impact the bacterial
53 community in the gut. These include antimicrobial peptides, toxic metals (*e.g.* copper),
54 reactive oxygen species (ROS), reactive nitrogen species (RNS), and reactive chlorine
55 species (RCS) (3, 13, 14). Since bacteria living in an inflamed gut are likely to be
56 exposed to substantially increased levels of these toxins, the differential survival of
57 proteobacteria during long-term inflammation suggests that *E. coli* may have evolved
58 better mechanisms to resist these stresses than other types of commensal bacteria.
59 Innate immune cells use copper as an antimicrobial agent and copper levels rise
60 in inflamed tissues, although the exact mechanism(s) by which copper kills bacteria are
61 not yet fully understood (15-17). RCS are highly reactive oxidants produced by
62 neutrophils and are potent antibacterial compounds (18, 19) that have been reported to
63 play a role in controlling intestinal bacterial populations (20-22). *E. coli* does not
64 efficiently survive being phagocytosed by neutrophils (23, 24), but the release of RCS-
65 generating myeloperoxidase from neutrophils in the inflamed gut (11) means that *E. coli*
66 is exposed to increased levels of RCS in that environment. The RCS response of *E. coli*
67 is complex and incompletely understood (19, 25-28), but characteristically involves
68 repair of damaged cellular components, often proteins (19). Protein-stabilizing
69 chaperones are upregulated during RCS stress, including Hsp33 (29, 30) and inorganic
70 polyphosphate (28, 31, 32), and enzymes are expressed that repair oxidized proteins,

71 including periplasmic methionine sulfoxide reductase (MsrPQ) (33) and the
72 chaperedoxin CnoX (34). *E.* coli has multiple HOCl-sensing regulators, including
73 YedVW (which regulates MsrPQ) (33), NemR (regulator of NemA and GloA, which
74 detoxify reactive aldehydes) (25), HypT (which regulates cysteine, methionine, and iron
75 metabolism) (27), and RclR, the RCS-specific activator of the *rclABC* operon (26).
76 The *rclA* gene of *E. coli* encodes a predicted flavin-dependent oxidoreductase, is
77 upregulated more than 100-fold in the presence of RCS (26, 35), and protects against
78 killing by HOCl via a previously unknown mechanism (26). RclA is the most
79 phylogenetically conserved protein of the Rcl system (Figure 1) and is found almost
80 exclusively in bacteria known to colonize epithelial surfaces (Supplemental Table 1),
81 suggesting that it may play an important role in host-microbe interactions in many
82 species. Bacteria encoding RclA homologs include Gram negative species (*e.g.*
83 *Salmonella enterica*), Gram positive species (*e.g. Streptococcus sanguinis*), obligate
84 anaerobes (*e.g. Clostridium perfringens*), facultative anaerobes (*e.g. Staphylococcus*
85 *aureus*), pathogens (*e.g. Enterococcus faecalis*), commensals (*e.g. Bacteroides*
86 *thetaiotaomicron*), and probiotics (*e.g. Lactobacillus reuteri*) (36), suggesting that RclA's
87 function may be broadly conserved and not specific to a single niche or type of host-
88 microbe interaction. RclR, RclB, and RclC are much less widely conserved, and are
89 found only in certain species of proteobacteria, primarily members of the
90 *Enterobacteriaceae* (Figure 1 and Supplemental Table 1).

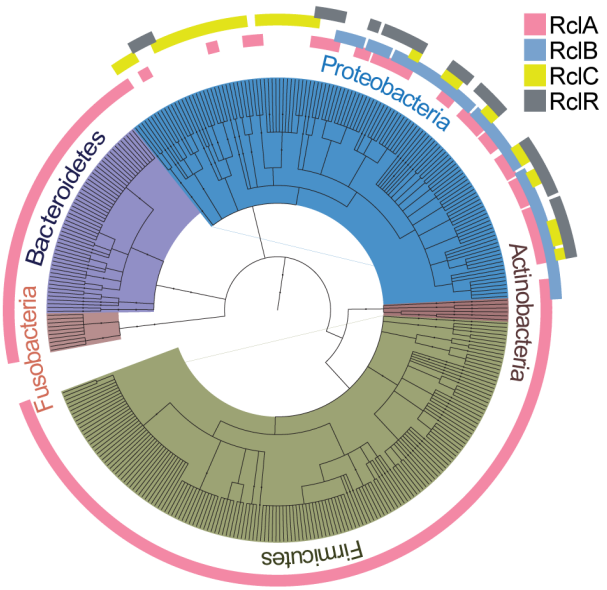

91

92 **Figure 1: RclA is widely conserved among bacteria that colonize epithelial**
93 **surfaces.** Phylogenetic tree made from amino acid sequence alignments of RclA (284
94 species), RclB (61 species), RclC, (49 species), and RclR (43 species), relative to the
95 respective proteins in *E. coli* MG1655. See Supplemental Data Table 1 for lists of each
96 hit used in the phylogenetic tree. Tree graphic was made using the interactive tree of life
97 (37).

98

99 In this work, we have now determined that RclA is a thermostable, HOCl-
100 resistant copper (II) reductase that is required for efficient colonization of an animal host
101 and protects *E. coli* specifically against the combination of HOCl and intracellular
102 copper, probably by preventing the formation of highly reactive Cu(III). We also found
103 that, surprisingly, extracellular copper effectively protects bacteria against killing by
104 HOCl both in cell culture and in an animal colonization model, most likely by catalyzing
105 the breakdown of HOCl before it reaches the bacterial cells. These findings reveal a
106 previously unappreciated interaction between two key inflammatory antimicrobials and a

107 novel way in which a commensal bacterium responds to and resists the combinatorial
108 stress caused by copper and HOCl.
109

110 RESULTS

111 **RclA contributes to HOCl resistance and host colonization.** An *rclA* mutant of *E.*
112 *coli* is more susceptible to HOCl-mediated killing than the wild-type (26). In this work,
113 we utilized a growth curve-based method to measure sensitivity to sub-lethal HOCl
114 stress by quantifying changes in lag phase extension (LPE) of cultures grown in the
115 presence of HOCl. Using this method, which we have found to be considerably more
116 reproducible than other techniques for assessing bacterial HOCl sensitivity, we
117 observed significant increases in LPE for a Δ*rclA* mutant strain compared to the wild
118 type grown in the presence of various concentrations of HOCl (Supplemental Figure 1).
119 We observed similar trends when the assay was done on stationary- and log-phase
120 cells (Supplemental figure 2A and B), so stationary phase cultures were used for
121 subsequent assays. Furthermore, we determined that there was no drop in CFU after
122 treatment with HOCl at these concentrations, indicating that LPE measures recovery of
123 cultures from non-lethal stress (Supplemental figure 2C). These results confirm previous
124 results and further illustrate the importance of RclA in resisting HOCl-mediated oxidative
125 stress in *E. coli*.

126 To directly test the role of RclA in interactions with an animal host, we examined
127 the ability of *E. coli* to colonize the intestine of *Drosophila melanogaster*, where the
128 presence of enterobacteria is known to stimulate antimicrobial HOCl production by the
129 dual oxidase Duox (20, 22). Since an *E. coli* K-12 strain did not efficiently colonize *D.*

130 *melanogaster* (Supplemental Figure 3), we used the colonization-proficient *E. coli* strain
131 Nissle 1917 (EcN) (38, 39) in these experiments. EcN Δ*rclA* mutants had a significant
132 defect in their ability to colonize NP1-GAL4 *D. melanogaster* flies compared to wild-type
133 EcN at 3- and 8-hours post infection (hpi) (Figure 2, filled circles). This shows that *rclA*
134 is important for EcN to survive host responses during early colonization.
135 To investigate the role of host-produced RCS in the colonization defect of the
136 *rclA* EcN mutant, we reduced the gut-specific expression of Duox in the flies using
137 Duox-RNAi and repeated the colonization experiments. Both strains colonized
138 significantly better at 3 hpi when Duox was knocked down in the flies (Figure 2, x
139 symbols), which was expected because *rclA* is not the only gene known to contribute to
140 HOCl resistance in *E. coli* (19). Importantly, the colonization defect of Δ*rclA* EcN at 3 hpi
141 was abrogated in the *DuoxIR* flies, with CFUs/fly not being significantly different from
142 wild-type EcN colonizing flies that are able to express Duox in the gut (Figure 2). We
143 confirmed that HOCl production was reduced in the *DuoxIR* flies using the HOCl-
144 sensing fluorescent probe R19-S (Supplemental Figure 4) (40). Taken together, these
145 results show that *rclA* facilitates colonization of an animal host during early timepoints
146 and indicate that *rclA* relieves stress caused by host-produced oxidation.
147

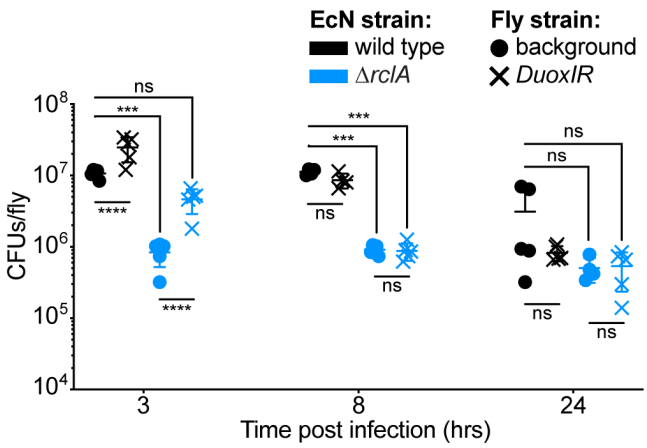

148

149 **Figure 2: EcN lacking *rclA* colonize *D. melanogaster* less effectively and early**

150 **colonization with Δ*rclA* EcN is improved in the absence of Duox-mediated**

151 **oxidation.** Flies were fed either wild-type or Δ*rclA* EcN ($1x10^{11}$ CFU/mL) and bacterial

152 loads were measured at the indicated times post infection (n = 4 - 5, ± SD). RCS-

153 deficient Duox-RNAi flies were obtained from crosses of *UAS-dDuox-RNAi* with *NP1-*

154 *GAL4* (enterocyte - specific driver). Statistical analysis was performed using a two-way

155 ANOVA with Tukey's multiple comparisons test (**** = P < 0.0001, *** = P < 0.001, ns =

156 not significant).

157

158 **RclA is homologous to mercuric reductase (MerA) and copper response genes**

159 **are upregulated after HOCl stress in EcN.** Although the fact that *rclA* protects *E. coli*

160 from RCS was previously known (26), the mechanism by which it does so was not.

161 Based on its homology to other flavin-dependent disulfide oxidoreductases (41), we

162 hypothesized that RclA catalyzed the reduction of an unknown cellular component

163 oxidized by RCS. RclA is homologous to mercuric reductase (MerA), an enzyme that

164 reduces Hg(II) to Hg(0) (42). These sequences are particularly well conserved at the

165 known active site of MerA, a CXXXXC motif (Figure 3). However, MerA has an extra N-

166 terminal domain and two additional conserved cysteine pairs used in metal binding (42)
167 while RclA only has one conserved cysteine pair (Supplemental Figures 5 and 6). This
168 indicates that if RclA does interact with metal(s), those interactions must be mediated
169 through mechanisms different from those of MerA.
170

171

172 **Figure 3: RclA and Mercuric reductase (MerA) share a conserved active site.**
173 Active site alignment of *E. coli* RclA and MerA amino acid sequences from seven
174 bacterial species (*Escherichia coli*, *Staphylococcus aureus*, *Salmonella enterica*,
175 *Listeria monocytogenes*, *Klebsiella pneumoniae*, *Serratia marcescens)*. Alignment was
176 made using CLUSTAL O (1.2.4) and graphic was made with WEBLOGO.
177

178 HOCl-stressed *E. coli* K-12 downregulates genes encoding iron import systems
179 (*e.g. fepABCD, fhuACDF*) and upregulates genes for zinc and copper resistance (*e.g.*
180 *copA, cueO, cusC, zntA, zupT*) (25), also suggesting metals may play some role in RCS
181 resistance. Transcriptomic profiling of EcN after treatment with a sublethal dose of HOCl
182 confirmed this and revealed the upregulation of several genes encoding proteins
183 involved in response to copper toxicity (Figure 4, Supplemental Table 2), despite the
184 very low amounts of copper present in the media used in that experiment (9 nM) (43).
185 These include members of the Cus and Cue export systems, which are factors
186 appreciated for their role in preventing copper toxicity and importance for *E. coli*
187 colonization within mammalian hosts (44-47). This suggested that copper might play an

188 important role during HOCl stress for EcN. The homology between RclA and MerA and
189 the indication that copper and HOCl responses may be connected in *E. coli* led us to
190 investigate the role of *rclA* in resisting HOCl stress under growth conditions containing
191 different amounts of copper.
192

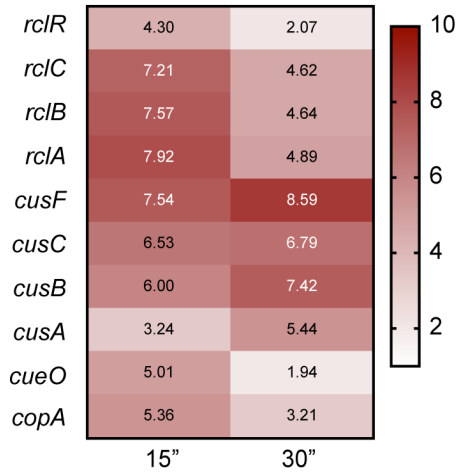

193
194 **Figure 4: EcN upregulates copper export proteins during HOCl stress.** Log_2 fold-
195 change in EcN gene expression at 15 and 30 minutes after non-lethal HOCl treatment
196 (0.4 mM), relative to a control sample taken directly before treatment. mRNA counts
197 were measured using RNA sequencing and analyzed with Bowtie2.
198
199 **Extracellular $CuCl_2$ protects both wild-type and Δ*rclA E. coli* against HOCl.** How
200 the presence of copper influences bacterial sensitivity to RCS has not been investigated
201 before this study. We first used growth curves in the presence of copper and HOCl to
202 identify how combinations of HOCl and extracellular copper influenced the sensitivity of
203 wild type and Δ*rclA* mutant *E. coli* (Figure 5A and 5B). As we observed above, the Δ*rclA*
204 mutant was more sensitive to HOCl in MOPS, but the sensitivity to HOCl of both strains

205 was greatly increased when Cu was removed from the media, indicating that the low
206 concentration of Cu present in MOPS medium (9 nM) (43) was enough to react with the
207 added HOCl and change the sensitivity of our strains. Consistent with this and the ability
208 of Cu to catalyze the decomposition of HOCl to non-toxic O_2 and Cl^- (48-51), addition of
209 10 μM $CuCl_2$ to HOCl-containing media greatly decreased sensitivity of both the wild
210 type and the *rclA* null mutant to HOCl (Figure 5). Copper being uniformly protective for
211 both strains makes it likely that extracellular copper had reacted with and detoxified the
212 HOCl before cells were inoculated into the media. To confirm this result, we tested if the
213 addition of exogenous copper (0.5 mM $CuCl_2$) could protect *E. coli* against killing by a
214 very high concentration of HOCl (1 mM). We found that treatment with 1 mM HOCl
215 resulted in complete killing of both strains (Figure 5C). Both strains survived several
216 orders of magnitude better when 0.5 mM $CuCl_2$ was added to the media immediately
217 before HOCl stress (Figure 5C). In addition, colonization of flies by EcN was enhanced
218 when their diet was supplemented with copper (Supplemental Figure 8), consistent with
219 Cu detoxifying HOCl *in vivo*. Taken together, these results illustrate that the presence of
220 exogenous copper strongly protects *E. coli* against HOCl.
221

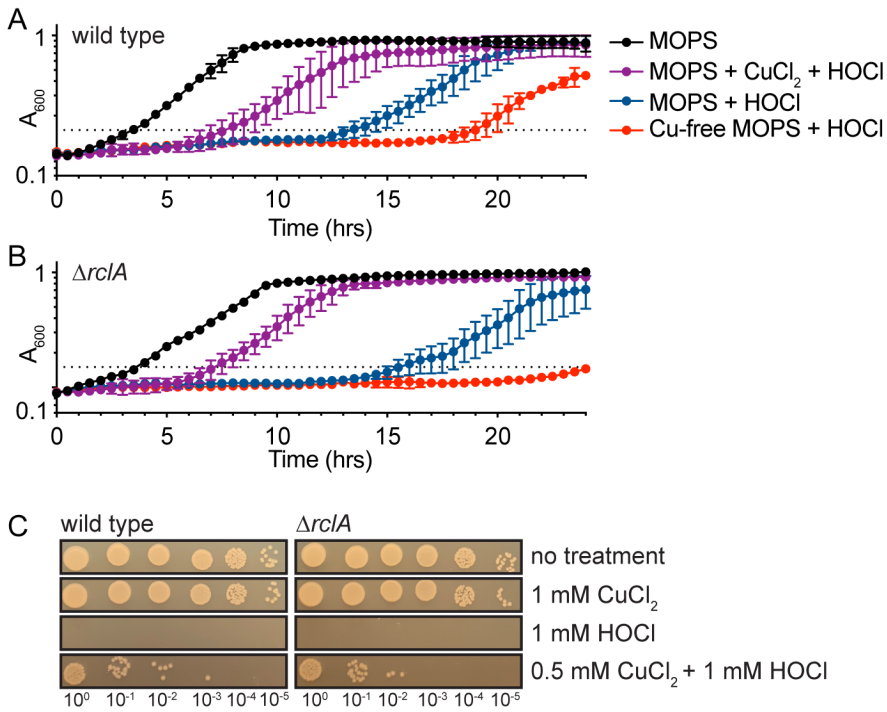

Figure 5: Extracellular $CuCl_2$ protects both wild-type and Δ*rclA* *E. coli* against HOCl. Growth curves of wild type (A) and Δ*rclA* (B) strains in MOPS with the addition of various combinations of HOCl (132 μM) and $CuCl_2$ (10 μM) (n = 3, ± SD for each treatment). Only one of several HOCl concentrations tested is shown for simplicity, see Supplemental Figure 7 for lag phase extension calculations and a summary of all the conditions tested using the growth curve method. (C) Exogenous copper protects both wild type and Δ*rclA* *E. coli* from lethal HOCl stress (10 min at 1 mM).

RclA protects *E. coli* against the combination of HOCl and intracellular copper. Next, we aimed to investigate how intracellular copper affects the HOCl resistance of *E coli*. To address this, we grew wild type and Δ*rclA* mutant *E. coli* overnight in minimal media with or without copper before inoculating the strains into copper-free media to perform HOCl-stress growth curves. Growing overnight cultures in media lacking copper

236 was expected to starve the cells for this metal, thereby reducing the concentration of
237 intracellular copper in those cultures. A broad range of HOCl concentrations were
238 assayed to account for quenching of the oxidant by media components.

239 Consistent with the results in Figure 5, *E. coli* was more sensitive to inhibition by
240 HOCl in media without copper. The Δ*rclA* mutant was more sensitive to HOCl than the
241 wild type when grown overnight in copper-containing media, but this phenotype was lost
242 when cells were starved for copper before stress (Figure 6), indicating that the
243 physiological role of RclA is to resist the stress resulting from the combination of HOCl
244 and copper in the cytoplasm.

245

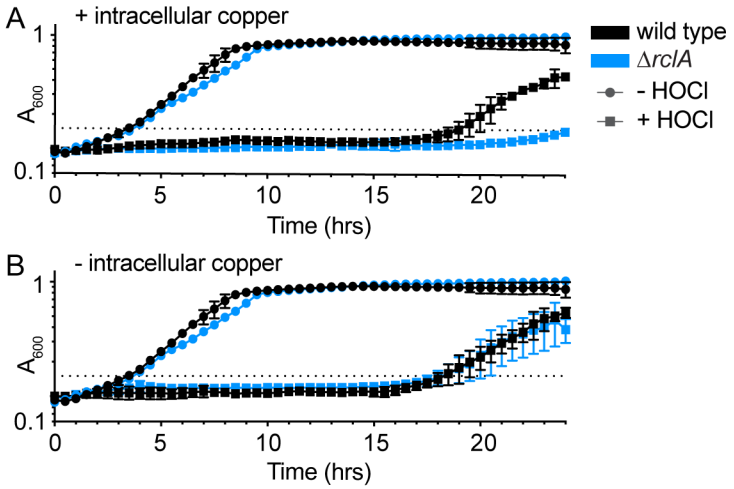

246

247 **Figure 6: *rclA* is required to resist the combination of HOCl and intracellular Cu.**
248 HOCl (132 μM) growth curves (n = 3, ± SD) in copper-free MOPS of wild-type and Δ*rclA*
249 *E. coli* after being grown up overnight in MOPS with (A) and without copper (B). Copper-
250 free MOPS was prepared by treating the media with Chelex-100™ Chelating Resin
251 (Bio-Rad 1421253) and adding back all the metals (metal stock solutions prepared in
252 metal-free water, Optima™ LC/MS Grade, Fisher Chemical W6-1), except for copper, to

253 the published concentrations (43). In cells containing intracellular copper (A), the Δ*rclA*
254 mutant has delayed growth relative to the wild type. There is no difference between the
255 strains when the cells are starved for intracellular copper (B). One HOCl concentration
256 is shown for simplicity, see Supplemental Figure 9 for growth curves showing more
257 HOCl concentrations.
258
259 **RclA reduces copper (II) to copper (I).** Based on the effect of copper starvation on the
260 HOCl sensitivity of the Δ*rclA* mutant, the sequence homology between RclA and MerA,
261 and the predicted oxidoreductase activity of RclA (41), we hypothesized that the
262 substrate of RclA might be copper. The reaction between copper and HOCl is known to
263 generate strong oxidizing intermediates, most likely highly reactive Cu(III) (48-52). HOCl
264 is also capable of oxidizing other transition metals, including iron (53, 54) and
265 manganese (55, 56). We therefore measured the specific activity (SA) of purified RclA
266 in the presence of a panel of biologically relevant metals. We also included mercury in
267 the panel of metals because of RclA's homology to MerA, although it is unlikely to be
268 physiologically relevant since we do not expect *E. coli* to encounter this metal in its
269 environment under normal conditions. We note that the oxidized forms of many
270 transition metals are insoluble in aqueous solution, which limited the set of substrates
271 we could test with this experiment.
272 In the absence of any metal, RclA slowly oxidized NADH (0.0303 μmole NAD^+
273 min^{-1} mg^{-1} RclA), consistent with the background activity of other flavin-dependent
274 oxidoreductases in the absence of their specific substrates (57, 58). Three of the metals
275 we tested significantly affected RclA SA, as measured by NADH oxidation. Copper and

276 mercury both significantly increased the SA of RclA, while zinc caused a decrease in SA
277 (Figure 7A). Copper is a potent inhibitor of MerA activity (59), further emphasizing the
278 distinct nature of these two enzymes. RclA oxidized NADPH at similar rates to NADH in
279 the absence of metals, but there was no significant increase to SA when copper was
280 added to the reactions. The addition of exogenous thiols, commonly added as β-
281 mercaptoethanol (BME), is required for MerA activity (60). To determine if exogenous
282 thiols increase the reaction rate of RclA, we added 1 mM BME to the RclA reactions.
283 BME rapidly reduced Cu(II) to Cu(I) in the absence of RclA, but had no effect on the SA
284 of NADH reduction by RclA with or without the addition of copper (Supplemental Figure
285 10).

286 Since RclA is an NADH oxidase, the results shown in Figure 7A strongly
287 suggested that this enzyme was concurrently reducing copper. Copper exists in four
288 possible oxidation states, Cu(I), Cu(II), and the less common and highly reactive Cu(III)
289 and Cu(IV) states (61). The copper salt used in our RclA SA determinations was $CuCl_2$,
290 suggesting that RclA was reducing this Cu(II) species to Cu(I). This was very surprising,
291 since Cu(I) is generally thought of as a toxic species that causes oxidative stress (46,
292 62), so it was not obvious either why *E. coli* would produce Cu(I) during RCS stress or
293 why production of Cu(I) might be protective. We therefore first sought to validate that
294 RclA was in fact reducing Cu(II) to Cu(I) while oxidizing NADH to NAD^+. We measured
295 Cu(I) accumulation in RclA reactions directly using the Cu(I)-specific chelator
296 bathocuproinedisulfonic acid (BCS) (63). NADH spontaneously reduces Cu(II) (64) at
297 rates too slow to impact the measurements made here, but BCS increases the rate of
298 this non-enzymatic copper reduction by shifting the equilibrium of the reaction towards

299 Cu(I) (65). Stopping RclA reactions with a mixture of BCS and EDTA, to chelate any
300 remaining Cu(II), allowed us to observe RclA-dependent Cu(I) accumulation
301 (Supplemental Figure 11). We observed a significant increase in BCS/Cu(I) complex
302 formation only in reactions containing RclA, NADH, and Cu(II), and not in reactions
303 lacking any single component (Figure 7B, Supplemental Figure 11). Furthermore, we
304 validated that the copper reductase activity of RclA was maintained when the reactions
305 were performed anaerobically (Supplemental Figure 12) and that FAD alone did not
306 catalyze Cu(II) reduction (Figure 7A). Taken together, these findings show that RclA has
307 Cu(II) reductase activity and generates Cu(I) as a product.
308

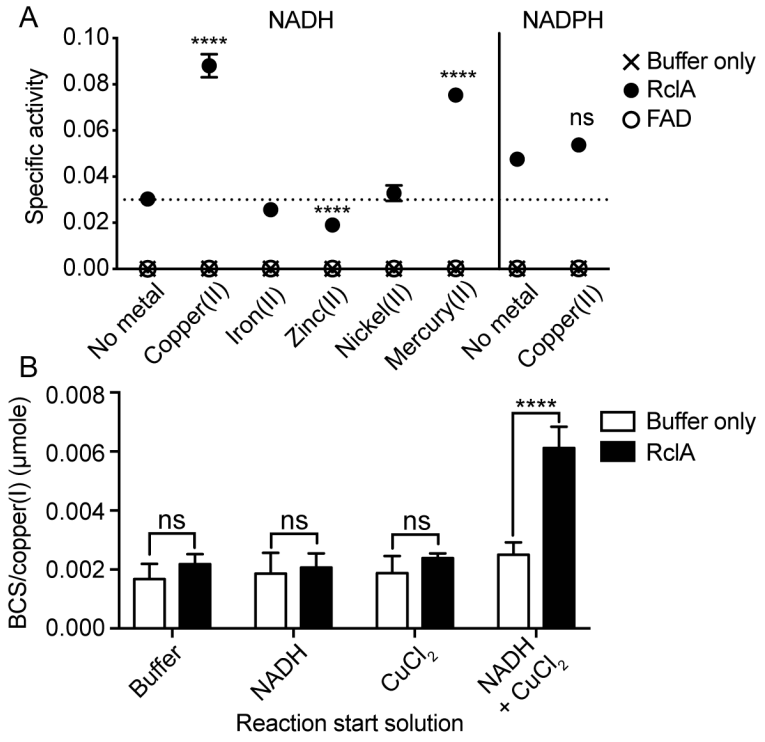

309

310 **Figure 7: RclA reduces Cu(II) to Cu(I).** (A) RclA specific activity (SA) increases in the
311 presence of Cu(II) and Hg(II). SA (μmole $NAD(P)^+$ min^{-1} mg^{-1} RclA) of RclA was assayed
312 by measuring NAD(P)H oxidation over time spectrophotometrically (n = 6, ± SD).

313 Differences in SA in the presence of each metal were analyzed using a two-way
314 ANOVA with Dunnet's multiple comparison test using the no metal reaction as the
315 control (****= P < 0.0001, ** = P < 0.01). (B) Cu(I) accumulates after the RclA and
316 NADH/copper (II) reaction, as measured by BCS/Cu(I)-complex absorption. RclA
317 reactions were started with the indicated solutions and carried out as described in A (n =
318 6, ± SD). Differences in the amount of BCS/Cu(I) complex between the buffer only and
319 RclA reactions were analyzed using a two-way ANOVA with Dunnet's multiple
320 comparison test using the buffer only sample as the control for each reaction start
321 solution (****= P < 0.0001, ns = not significant).
322
323 **RclA does not protect against HOCl by facilitating copper export.** Since the copper
324 exporters of *E. coli* (*copA* and *cusCFBA*) are upregulated by HOCl treatment (Figure 3,
325 Supplemental Table 2) (25) and only transport Cu(I) (46, 47, 66, 67), it was possible that
326 RclA facilitates the rapid export of cytoplasmic copper, allowing it to react with and
327 eliminate HOCl outside the cell. To test whether the Cu(II) reductase activity of RclA is
328 important for exporting copper during HOCl stress, we measured intracellular copper
329 concentrations before and after HOCl stress with ICP mass spectrometry. We found
330 that the Δ*rclA* mutant contained, on average, more intracellular copper before HOCl
331 stress than the wild-type but that both strains contained similar amounts of copper after
332 HOCl stress (Supplemental Figure 13). We constructed mutants lacking *copA*, which is
333 reported to result in increased intracellular copper (47), but unexpectedly found that the
334 *copA rclA* double mutant had a substantial growth defect in copper-free media, even in
335 the absence of HOCl (Supplemental Figure 14). We do not yet know the explanation for

336 this intriguing result. Overall, our results indicate that although RclA may affect basal
337 copper homeostasis, it does not appear to protect *E. coli* against HOCl by facilitating
338 export of copper at levels detectable using these methods.
339
340 **RclA is thermostable and resistant to denaturation by HOCl and urea.** We
341 hypothesized that the copper reductase activity of RclA was likely to be relatively stable
342 under denaturing conditions because it must remain active during exposure to HOCl
343 stress, which is known to cause extensive protein misfolding and aggregation *in vivo*
344 (19, 27, 28, 32-34). To test this hypothesis, we first measured RclA activity after
345 treatment with protein denaturing agents (HOCl and urea) *in vitro*. HOCl treatment (with
346 0, 5, 10, and 20-fold molar ratios of HOCl to RclA) was done on ice for 30 minutes and
347 urea treatment (0, 2, 4, and 6 M) was carried out at room temperature for 24 hours.
348 RclA retained full copper reductase activity at all HOCl levels tested, indicating that it is
349 highly resistant to treatment with HOCl (Figure 8A). By comparison, the NADH oxidase
350 activity of lactate dehydrogenase was significantly decreased after treatment with a 5-
351 fold excess of HOCl (Figure 8B). RclA also retained a remarkable 35.8% of full activity
352 after being equilibrated in 6 M urea (Figure 8C). Finally, we used circular dichroism (CD)
353 spectroscopy to measure the melting temperature (T_m) of RclA, which was 65 °C
354 (Figure 8D, Supplemental Figure 15), indicating that RclA is thermostable relative to the
355 rest of the *E. coli* proteome, which has an average T_m of 55 °C (standard deviation = 5.4
356 °C) (49, 68).
357

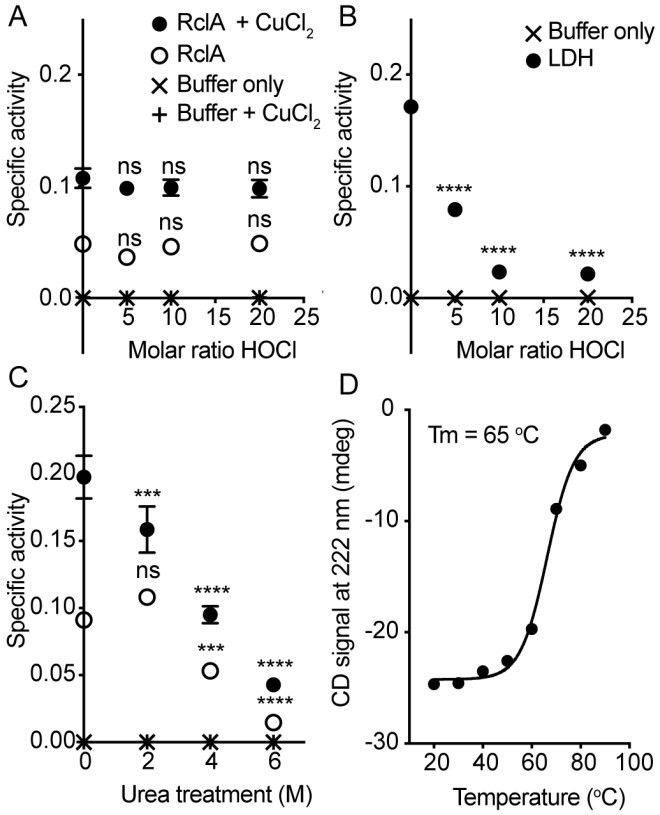

358

359 **Figure 8. RclA is resistant to denaturation.** (A) SA of RclA (μmoles NAD^+ min^{-1} mg

360 $RclA^{-1}$), with and without $CuCl_2$, after being treated with the indicated molar ratios of

361 HOCl to RclA. (B) SA of lactate dehydrogenase (LDH) (μmoles NAD^+ min^{-1} U LDH^{-1})

362 used as control reactions for HOCl degradation of enzymatic activity. (C) RclA with and

363 without $CuCl_2$ (200 μM final) after being treated with the indicated concentrations of

364 urea. (D) CD signals at 222 nm (mdeg) (raw data shown in Supplemental Figure 15) at

365 each temperature used to determine the T_m of RclA (65 ˚C). Differences in SA (n = 6, ±

366 SD) after treatment were analyzed using a two-way ANOVA with Sidak's multiple

367 comparison test for HOCl treatment (A and B) and Dunnet's test using the buffer only

368 reaction as the control for the urea treated samples (C) (**** = P < 0.0001, * = P < 0.05

369 ns = not significant).

370

371 DISCUSSION

372 The antimicrobial function of copper in host-microbe interactions is well-
373 established (15, 17, 44, 69), although the exact mechanism(s) by which copper kills
374 bacteria remain incompletely known (70, 71). In this work, we identified a new way in
375 which copper toxicity contributes to host-bacteria interactions via its reactions with RCS.
376 We identified RclA as a highly stable Cu(II) reductase (Figure 7) required for resisting
377 killing by the combination of HOCl and intracellular copper in *E. coli* (Figure 6). In the
378 absence of *rclA*, *E. coli* had a significant defect in the early stages of host colonization
379 which was partially eliminated when production of HOCl by the host was reduced
380 (Figure 2). Duox activation and HOCl production are rapid host responses that occur at
381 early stages of bacterial colonization of the gut (20), in agreement with our data showing
382 that RclA is important for initial establishment. As the course of infection progresses,
383 additional antimicrobial effectors, such as antimicrobial peptides regulated by NF-κB
384 signaling, become more prominent (27), which could explain the similar colonization
385 levels of mutant and wild-type strains at later time points. The amount of copper in
386 bacterial cells is low (15, 16), but how much is unbound by protein and its redox state
387 under different conditions are unknown (15). Given the broad conservation of RclA
388 among host-associated microbes, we propose that there is likely to be a common and
389 previously unsuspected role for copper redox reactions in interactions between bacteria
390 and the innate immune system.

391 Copper accumulates in host tissues during inflammation (72, 73), as do RCS (74,
392 75). Our discovery that even very low concentrations of extracellular copper can protect
393 bacteria against RCS both *in vitro* and *in vivo* adds a new and important facet to

394 understanding copper's role in innate immunity. Since a large proportion of host tissue
395 damage during inflammation is due to HOCl (76, 77), the presence of copper in
396 inflamed tissues may play an important role not only in killing bacteria, but potentially in
397 protecting host cells, although this hypothesis will require further testing. Our results
398 also show that media copper concentrations are a key variable in experiments testing
399 the sensitivity of cells to HOCl, and that care must be taken to account for media copper
400 content and use metal-free culture vessels in such experiments.

401 Both HOCl and copper cause oxidative stress in bacteria and Cu(I) is generally
402 considered more toxic than Cu(II) (15, 19, 44, 69, 70, 78), so we were surprised that a
403 Cu(II) reductase protected *E. coli* against HOCl. Copper reacts with the ROS hydrogen
404 peroxide (H_2O_2) to form highly reactive hydroxyl radicals (17, 45, 62, 71), but how the
405 presence of copper influences bacterial sensitivity to RCS has not been investigated
406 before this study. The chemistry of reactions between HOCl and copper is complicated.
407 HOCl can oxidize Cu(II) to highly reactive Cu(III) (48-52) and both Cu(I) and Cu(II) are
408 known to catalyze the breakdown of HOCl (48-51). At near-neutral pH, similar to that in
409 the large intestine or bacterial cytoplasm, Cu(I) accelerates the rate of decomposition of
410 HOCl to O_2 and chloride ions by as much as 10^8-fold (49). One possibility to explain the
411 protective effect of RclA is that it might facilitate an HOCl-degrading Cu(I) / Cu(II) redox
412 cycle in the cytoplasm. If this were the case, however, the Δ*rclA* mutant would become
413 more sensitive to HOCl in the absence of copper, the opposite of what we actually
414 observed (Figure 6). We therefore propose that RclA-catalyzed reduction of Cu(II) to
415 Cu(I) likely acts to limit the production of Cu(III) in the cytoplasm. Uncontrolled
416 production of Cu(III) could greatly potentiate the ability of HOCl to kill bacterial cells.

417 While RclA itself is widely conserved, the *rclABCR* locus as a whole is restricted
418 to certain enteric proteobacteria, including *E. coli*, *Salmonella*, *Citrobacter*, *Raoultella*,
419 *Serratia*, and *Shigella*. These genera are notable for their close association with gut
420 inflammation and the ability of pathogenic strains to bloom to very high levels in the gut
421 in disease states (2, 3, 7-10, 79, 80). We hypothesize that the ability to survive
422 increased levels of antimicrobial compounds (including RCS) in the inflamed gut is
423 important for the ability of enterobacteria to exploit this niche, and our *in vivo* results
424 with the Δ*rclA* mutant support this idea (Figure 2). The rate at which RclA oxidized
425 NADH in the presence of copper *in vitro* was slow (approximately 4.4 min^{-1}) (Figure 7),
426 suggesting that we have not yet identified optimal reaction conditions for this enzyme.
427 However, expression of *rclA* is rapidly induced >100-fold after sublethal doses of HOCl
428 in *E. coli* (Figure 3, Supplemental Table 2) (26), which could compensate *in vivo* for the
429 slow rate of NADH turnover we observed *in vitro*. We also do not currently know the
430 physiological roles of RclB, which is a small predicted periplasmic protein, or RclC,
431 which is a predicted inner membrane protein, although deletion of either of these genes
432 results in increased HOCl sensitivity in *E. coli* (26). We hypothesize that they may form
433 a complex with RclA *in vivo* and enhance its copper-dependent activity and are currently
434 pursuing experiments to test this idea.
435

436 EXPERIMENTAL PROCEDURES

437 ***Strain and plasmid construction.*** *E. coli* strain MJG0586 (F^-, λ^-, *rph-1 ilvG⁻ rfb-50*
438 Δ*rclA* λ(DE3 [*lacI lacUV5*-T7 gene 1 *ind1 sam7 nin5*])) was generated from MJG0046
439 (F^-, λ^-, *rph-1 ilvG⁻ rfb-50* Δ*rclA*) (26) using the Novagen DE3 lysogenization kit,

440 according to the manufacturer's instructions. The RclA coding sequence (1374 bp) was
441 amplified from *E. coli* MG1655 genomic DNA with primers 5' CTC GGT CTC CAA TGA
442 ATA AAT ATC AGG CAG TGA 3' and 5' CTC GGT CTC AGC GCT TTA TTT GAC TAA
443 TGA AAA TAG ATC A 3' and cloned into the *Eco*31I (*Bsa*I) sites of plasmid pPR-IBA101
444 (IBA Lifesciences) to yield plasmid pRCLA10. pRCLA11 was generated by using
445 QuikChange site directed mutagenesis (Agilent), modified to use a single mutagenic
446 primer (5' CTA TTT TCA TTA GTC AAA AGC GCT TGG AGC CAC CC 3'), to remove
447 the stop codon between the RclA coding sequence and the twin-strep tag sequence in
448 pRCLA10. *E. coli* Nissle 1917 Δ*rclA*::*cat*$^{+}$ strain MJG0846 was made by recombineering
449 (81) using primers 5' CGT CTA TAG TCA TGA TGT CAA ATG AAC GCG TTT CGA
450 CAG GAA ATC ATC ATG GTG TAG GCT GGA GCT GCT TC 3' and 5' CTT TTC TCT
451 GAG ACG CCA GAA TAT TTG TTC TGG CGT CTG ATT TTG AGT TTA CAT ATG
452 AAT ATC CTC CTT AG 3' to amplify the chloramphenicol resistance cassette from
453 pKD3. The *cat*$^{+}$ insertion was resolved using pCP20 resulting in the *E. coli* Nissle 1917
454 Δ*rclA* strain MJG0860.
455
456 ***Protein expression and purification.*** Expression of twin-strep tagged RclA was done
457 in MJG0586 containing pRCLA11 (MJG1338) in M9 minimal media (82) containing 2 g l^{-}
458 ^{1} glucose and 100 µg ml^{-1} ampicillin. Overnight cultures of MJG1338 were diluted 1:100
459 and grown up to A_{600} = 0.4 at 37 ˚C with shaking. When A_{600} = 0.4 was reached,
460 expression was induced with IPTG (1 mM final concentration) and allowed to continue
461 for 12-18 hours at 20 ˚C. Purification of recombinant RclA was achieved to high purity
462 using a 1 mL StrepTrap HP column (GE, 28-9136-30 AC) according to the

463 manufacturer's instructions. Purified protein was subsequently saturated with FAD
464 cofactor by incubating the protein preparation with a 10-fold molar excess of FAD at
465 room temperature for 45 mins. Excess FAD and elution buffer were dialyzed away with
466 three exchanges of 1 L of RclA storage buffer (50 mM Tris-HCl, pH 7.5, 0.5 M NaCl, 2
467 mM DTT, 10% glycerol) at 4 ˚C overnight.
468
469 ***Colonization of D. melanogaster with E. coli Nissle 1917.*** *D. melanogaster stocks*
470 *and husbandry: Canton-S* flies were used as a wild-type line. Duox-RNAi flies were
471 obtained from crosses of *UAS-dDuox-RNAi* with *NP1-GAL4* (gut-specific driver). Unless
472 otherwise noted, flies were reared on cornmeal medium (per liter of medium: 50g yeast,
473 70g cornmeal, 6g agar, 40g sucrose, 1.25ml methyl-paraben, and 5ml 95% ethanol).
474 *Oral infections:* Adult female flies were starved for 2h at 29˚C prior to being fed a 1:1
475 suspension of bacteria (OD_{600}=200) and 2.5% sucrose applied to a filter paper disk on
476 the surface of normal fly food. Suspensions of bacterial at OD_{600}=200 were consistently
477 found to contain $1x10^{11}$ CFU/mL (Supplemental Figure 16). A negative control was
478 prepared by substituting LB for the bacterial suspension. Infections were maintained at
479 29˚C. *CFU determination:* Flies were surface-sterilized in 70% ethanol and rinsed in
480 sterile PBS. Individual flies were homogenized in screw-top bead tubes containing 600µl
481 PBS. Dilution series of homogenates were prepared with a range of (10^0 to 10^{-5}). 3µl
482 spots of each dilution were applied to LB plates and grown overnight at 30˚C. *E. coli*
483 colonies were identified by morphology and counted to determine CFUs/fly.
484

485 ***RNA sequencing.*** *E. coli* Nissle 1917 was grown anaerobically (90% N_2, 5% CO_2, 5%
486 H_2, maintained with a Coy Laboratory Products anaerobic chamber) at 37°C in MOPS
487 minimal media (Teknova) in sealed Hungate tubes to an A_{600} = 0.25, then treated
488 anaerobically with 0.4 mM HOCl. Samples (7 ml) were harvested into 7 ml ice-cold
489 isopropanol immediately before and 15 or 30 minutes after HOCl addition, harvested by
490 centrifugation, and stored at -80°C until use. RNA was purified using the RiboPure™-
491 Bacteria Kit (Ambion), according to the manufacturer's instructions. mRNA-sequencing
492 was performed at the UAB Heflin Center for Genomic Sciences, using an Illumina
493 NextSeq 500 as described by the manufacturer (Illumina, Inc). The Agilent SureSelect
494 Strand Specific mRNA library kit (Agilent) and ribosome reduction with the RiboMinus
495 protocol for Gram-negative and Gram-positive bacteria (Life Technologies) were used
496 as described by the manufacturer. The resulting mRNA was randomly fragmented with
497 cations and heat, followed by first strand synthesis using random primers. Second
498 strand cDNA production was done with standard techniques, and cDNA libraries were
499 quantitated using qPCR in a Roche LightCycler 480 with the Kapa Biosystems kit for
500 Illumina library quantitation (Kapa Biosystems) prior to cluster generation, which was
501 performed according to the manufacturers recommendations for onboard clustering
502 (Illumina). We generated approximately 8 million double-stranded 50 bp reads per
503 sample. Data were analyzed using Bowtie2 and DEseq2. RNA sequencing data have
504 been deposited in NCBI's Gene Expression Omnibus (83) and are accessible through
505 GEO Series accession number GSE144068.
506

507 ***Growth curves for measuring sensitivity to HOCl.*** The molar HOCl concentration
508 from concentrated sodium hypochlorite (Sigma Aldrich 425044) was quantified by
509 measuring A_{292} of the stock solution diluted in 10 mM NaOH. Copper free MOPS was
510 prepared by removing total metals from MOPS minimal media (Teknova) containing 2 g
511 l^{-1} glucose and 1.32 mM K_2HPO_4 by treating prepared media with a universal chelator
512 (Chelex® 100 Chelating Resin, Bio-Rad 1421253), filtering sterilizing away the Chelex
513 resin, and adding back the metals normally present in MOPS suspended in metal-free
514 water, except for copper. Overnight cultures of MG1655 and MJG0046 were grown up
515 overnight in MOPS with and without copper. The overnight cultures were normalized to
516 A_{600} = 0.8 in and diluted to A_{600} = 0.08 in MOPS minimal medium without copper with the
517 indicated combinations/concentrations of HOCl and $CuCl_2$. Cultures were incubated
518 with shaking at 37 °C in a Tecan Infinite M1000 plate reader with A_{600} being measured
519 every 30 minutes for 27 hours. Sensitivity was subsequently determined by comparing
520 lag phase extensions (difference in hours to reach $A_{600} \geq 0.15$ from the no HOCl
521 treatment control under the same $CuCl_2$ condition) for each stress condition.
522
523 ***Determining the effect of copper on lethal HOCl stress.*** Wild type and Δ*rclA E.*
524 *coli* MG1655 were grown overnight in MOPS minimal media. 500 µl of the overnight
525 culture was pelleted, resuspended in copper-free MOPS, and subcultured into 9.5 ml of
526 copper-free MOPS, then grown with shaking at 37°C to mid-log phase (A_{600} = 0.3 - 0.4).
527 Once mid-log phase was reached, 1 mL of cells was aliquoted into microcentrifuge
528 tubes for each treatment. Cells were treated by adding the indicated amounts of copper
529 (II) chloride, followed by 1 mM HOCl, then incubated on a 37°C heat block for 10

530 minutes. After incubation, treatments were serially diluted in PBS and 5 µl aliquots were
531 spotted on LB agar plates. Plates were dried and incubated at room temperature for 2
532 days.
533
534 ***Measuring intracellular copper after HOCl stress.*** Wild-type and Δ*rclA E. coli* were
535 grown up to A_{600} = 0.6 in MOPS and stressed with 400 µM HOCl for 30 mins at 37 ºC
536 with shaking. After 30 mins, the cultures were diluted 2-fold with MOPs to quench HOCl
537 and pelleted. The mass of pellets was determined after being rinsed 3 times with PBS.
538 Amount of copper was measured via ICP-MS (Agilent Technologies 7700x ICP-MS,
539 Santa Clara, CA, USA) after suspending the collected pellets in concentrated nitric acid
540 and diluting the suspensions to a 2% nitric acid matrix. Samples were filtered through
541 0.22 µM polytetrafluoroethylene filters to remove any particulates before running
542 performing metal determination. Copper concentrations were determined by comparison
543 to a standard curve (Agilent, 5188-6525) as calculated by Agilent software (ICP-MS
544 MassHunter v4.3). Values determined by ICP-MS were normalized to pellet mass and
545 dilution factor.
546
547 ***NADH oxidase activity.*** Activity of purified RclA was assayed in 20 mM HEPES, 100
548 mM NaCl, pH 7 by measuring NADH oxidation over time spectrophotometrically.
549 Purified recombinant RclA was preloaded into wells of a 96 well plate (100 µL of 6 uM
550 RclA). Reactions were started by adding 100 µL of NADH (200 µM final) with the
551 indicated metal salts (200 µM final) to RclA (3 µM final) at 37 ºC. The absorbance of
552 NADH (A_{340}) was measured kinetically each minute for five minutes in a Tecan Infinite

553 M1000 plate reader. A_{340} values were then used to calculate μmoles of NADH (ε_{340} =
554 6300 M^{-1} cm^{-1}) and NADPH (ε_{340} = 6220 M^{-1} cm^{-1}) at each timepoint. Absolute values of
555 slopes of NAD(P)H (μmoles) over time (min) were divided by mg of RclA to determine
556 the reported specific activities (SA, μmole $NAD(P)^+$ min^{-1} mg^{-1} RclA) for each condition.
557
558 ***Copper (I) quantification.*** Cu(I) accumulation after the course of the RclA reaction was
559 measured using bathocuproinedisulfonic acid disodium salt (BCS, Sigma Aldrich
560 B1125). NADH oxidation reactions were carried out as in the previous section but were
561 started with either NADH (200 μM final), $CuCl_2$ (200 μM final), NADH and $CuCl_2$ (both at
562 200 μM final), or reaction buffer as a negative control to observe levels of background
563 copper in the reagents used. Each reaction was stopped at 5 minutes with a BCS (400
564 μM final) and EDTA (1 mM final) solution using the injector system of a Tecan Infinite
565 M1000 plate reader. The stopped reactions were incubated at 37 ºC with the
566 absorbance of BCS/Cu(I) complex being measured at 483 nm every minute for five
567 minutes to ensure complete saturation of the BCS. The amount of the BCS/Cu(I)
568 complex after 5 minutes was determined using the molar extinction coefficient 13,000
569 M^{-1} cm^{-1} (63).
570
571 ***NADH oxidase activity after treatment with urea and HOCl.*** SA of RclA after being
572 treated with denaturing agents was done by determining SA as above after incubation
573 of RclA with either urea or HOCl. Urea treatment was done on 3 μM RclA for 24 hours
574 at room temperature with increasing concentrations of urea (0, 2, 4, and 6 M) in reaction
575 buffer (20 mM HEPES, 100 mM NaCl, pH 7). HOCl treatment was done by mixing

576 increasing molar ratios of HOCl (0, 5, 10, and 20 X) with concentrated RclA or L -
577 Lactate Dehydrogenase (LDH, Sigma LLDH-RO 10127230001) (35 μM) in oxidation
578 buffer (50 mM sodium phosphate, pH 6.8, 150 mM NaCl) and incubating mixtures on ice
579 for 30 minutes. HOCl treatment was quenched after 30 minutes by diluting the RclA
580 solutions to 6 μM and the LDH solutions to 1 μM in reaction buffer (20 mM HEPES, 100
581 mM NaCl, pH 7). NADH oxidation reactions using LDH were performed under the same
582 conditions as the RclA reactions but started with 1.2 mM NADH and 1.2 mM pyruvate.

583

584 ***Melting temperature determination.*** Circular Dichroism (CD) spectra were obtained
585 on a Jasco J815 circular dichroism spectrometer. CD spectra were collected on purified
586 recombinant RclA exchanged into 20 mM HEPES, 100 mM NaCl, pH 7.5. Room
587 temperature CD spectra in the range of 260 nm to 190 nm were obtained in 0.1 mm
588 demountable quartz cells. Thermal CD data between 30 °C and 90 °C were obtained in
589 standard 1.0 mm quartz cells. All data were collected with a 1.0 nm step size, 8 second
590 averaging time per point, and a 2 nm bandwidth. Data were baseline corrected against
591 the appropriate buffer solution and smoothed with Jasco software.

592

593 ***Data analysis and bioinformatics.*** *Statistics*: All statistical analyses were performed
594 using GraphPad Prism (version 7.0a). *Phylogenetic tree*: RclA conservation tree was
595 made from amino acid sequence alignments of RclA (BLAST e value < $1x10^{-90}$ in 284
596 species), RclB (BLAST e value < $1x10^{-1}$ in 61 species), RclC, (BLAST e value < $1x10^{-80}$
597 in 49 species), and RclR (BLAST e value < $1x10^{-40}$ in 43 species). BLAST searches
598 were done by comparing to each respective protein in *E. coli* MG1655. Tree graphic

599 was made using the interactive tree of life (37) (https://itol.embl.de/). *Amino acid*
600 *sequence alignments*: Active site alignment of *E. coli* RclA (ADC80840.1) and MerA
601 amino acid sequences from seven bacterial species (*Escherichia coli*, ADC80840.1;
602 *Staphylococcus aureus*, AKA87329.1; *Salmonella enterica*, ABQ57371.1; *Listeria*
603 *monocytogenes*, PDA94520.1; *Klebsiella pneumoniae*, ABY75610.1; *Serratia*
604 *marcescens*, ADM52740.1). Alignment was made using CLUSTAL O (1.2.4)
605 (www.ebi.ac.uk/Tools/msa/clustalo/) and graphic was made with WEBLOGO
606 (weblogo.berkeley.edu/logo.cgi). Full length alignment of *E. coli* RclA (ADC80840.1)
607 and MerA (ADC80840.1). Alignment, conservation scoring, and graphic were made
608 using PRALINE (www.ibi.vu.nl/programs/pralinewww/).
609

610 ACKNOWLEDGEMENTS

611 Thanks to Dr. Peter Prevelige (UAB Department of Microbiology) for helpful
612 discussions, Emily Schwessinger (University of Michigan) for preliminary
613 characterization of RclA, Dr. Michael Jablonsky (UAB Chemistry Department) for
614 assistance with CD spectra acquisition, Dr. Won-Jae Lee (Seoul National University) for
615 providing the *D. melanogaster* Duox RNAi line, and William Van Der Pol and Ranjit
616 Kumar at the UAB Center for Clinical and Translational Science for their help with the
617 RNA sequencing analysis. This project was supported by University of Alabama at
618 Birmingham Department of Microbiology startup funds, NIH grant R35GM124590 (to
619 M.J.G), NIH grant R35GM128871 (to N.A.B.), and NIH training grant T90DE022736 (to
620 R.M.D).
621

622 CONFLICTS OF INTEREST

623 The authors have no conflicts of interest to declare.

624

625 AUTHOR CONTRIBUTIONS

626 R.M.D., A.J.B., C.E.B., and I.F.C. performed research, and R.M.D., A.J.B, S.E.L.,
627 N.A.B, and M.J.G. contributed to designing research, analyzing data, and writing the
628 paper.

629

630 REFERENCES

631 1. Kaplan GG (2015) The global burden of IBD: from 2015 to 2025. *Nat Rev*
632 *Gastroenterol Hepatol* 12(12):720-727.

633 2. Litvak Y, Byndloss MX, Tsolis RM, & Baumler AJ (2017) Dysbiotic Proteobacteria
634 expansion: a microbial signature of epithelial dysfunction. *Curr Opin Microbiol*
635 39:1-6.

636 3. Stecher B (2015) The Roles of Inflammation, Nutrient Availability and the
637 Commensal Microbiota in Enteric Pathogen Infection. *Microbiol Spectr* 3(3).

638 4. Manichanh C, Borruel N, Casellas F, & Guarner F (2012) The gut microbiota in
639 IBD. *Nat Rev Gastroenterol Hepatol* 9(10):599-608.

640 5. Casen C*, et al.* (2015) Deviations in human gut microbiota: a novel diagnostic
641 test for determining dysbiosis in patients with IBS or IBD. *Aliment Pharmacol*
642 *Ther* 42(1):71-83.

643 6. Dickson I (2017) Gut microbiota: Diagnosing IBD with the gut microbiome. *Nat*
644 *Rev Gastroenterol Hepatol* 14(4):195.

645 7. Litvak Y*, et al.* (2019) Commensal Enterobacteriaceae Protect against
646 Salmonella Colonization through Oxygen Competition. *Cell Host Microbe*
647 25(1):128-139 e125.
648 8. Zhu W*, et al.* (2018) Precision editing of the gut microbiota ameliorates colitis.
649 *Nature* 553(7687):208-211.
650 9. Lupp C*, et al.* (2007) Host-mediated inflammation disrupts the intestinal
651 microbiota and promotes the overgrowth of Enterobacteriaceae. *Cell Host*
652 *Microbe* 2(2):119-129.
653 10. Winter SE, Lopez CA, & Baumler AJ (2013) The dynamics of gut-associated
654 microbial communities during inflammation. *EMBO Rep* 14(4):319-327.
655 11. Wera O, Lancellotti P, & Oury C (2016) The Dual Role of Neutrophils in
656 Inflammatory Bowel Diseases. *J Clin Med* 5(12).
657 12. Park JH, Peyrin-Biroulet L, Eisenhut M, & Shin JI (2017) IBD
658 immunopathogenesis: A comprehensive review of inflammatory molecules.
659 *Autoimmun Rev* 16(4):416-426.
660 13. Chami B, Martin NJJ, Dennis JM, & Witting PK (2018) Myeloperoxidase in the
661 inflamed colon: A novel target for treating inflammatory bowel disease. *Arch*
662 *Biochem Biophys* 645:61-71.
663 14. Pavlick KP*, et al.* (2002) Role of reactive metabolites of oxygen and nitrogen in
664 inflammatory bowel disease. *Free Radic Biol Med* 33(3):311-322.
665 15. Braymer JJ & Giedroc DP (2014) Recent developments in copper and zinc
666 homeostasis in bacterial pathogens. *Curr Opin Chem Biol* 19:59-66.

667 16. Sheldo JR & Skaar EP (2019) Metals as phagocyte antimicrobial effectors.
668 *Current Opinion in Immunology* 60:1 - 9.
669 17. Besold AN, Culbertson EM, & Culotta VC (2016) The Yin and Yang of copper
670 during infection. *J Biol Inorg Chem* 21(2):137-144.
671 18. Winterbourn CC & Kettle AJ (2013) Redox reactions and microbial killing in the
672 neutrophil phagosome. *Antioxid Redox Signal* 18(6):642-660.
673 19. Gray MJ, Wholey WY, & Jakob U (2013) Bacterial responses to reactive chlorine
674 species. *Annu Rev Microbiol* 67:141-160.
675 20. Kim SH & Lee WJ (2014) Role of DUOX in gut inflammation: lessons from
676 Drosophila model of gut-microbiota interactions. *Front Cell Infect Microbiol* 3:116.
677 21. Ha EM, Oh CT, Bae YS, & Lee WJ (2005) A direct role for dual oxidase in
678 Drosophila gut immunity. *Science* 310(5749):847-850.
679 22. Lee KA*, et al.* (2013) Bacterial-derived uracil as a modulator of mucosal immunity
680 and gut-microbe homeostasis in Drosophila. *Cell* 153(4):797-811.
681 23. Staudinger BJ, Oberdoerster MA, Lewis PJ, & Rosen H (2002) mRNA expression
682 profiles for Escherichia coli ingested by normal and phagocyte oxidase-deficient
683 human neutrophils. *J Clin Invest* 110(8):1151-1163.
684 24. Hofman P*, et al.* (2000) Increased Escherichia coli phagocytosis in neutrophils
685 that have transmigrated across a cultured intestinal epithelium. *Infect Immun*
686 68(2):449-455.
687 25. Gray MJ, Wholey WY, Parker BW, Kim M, & Jakob U (2013) NemR is a bleach-
688 sensing transcription factor. *J Biol Chem* 288(19):13789-13798.

689 26. Parker BW, Schwessinger EA, Jakob U, & Gray MJ (2013) The RclR protein is a
690 reactive chlorine-specific transcription factor in Escherichia coli. *J Biol Chem*
691 288(45):32574-32584.
692 27. Drazic A*, et al.* (2013) Methionine oxidation activates a transcription factor in
693 response to oxidative stress. *Proc Natl Acad Sci U S A* 110(23):9493-9498.
694 28. Gray MJ*, et al.* (2014) Polyphosphate is a primordial chaperone. *Mol Cell*
695 53(5):689-699.
696 29. Dahl JU, Gray MJ, & Jakob U (2015) Protein quality control under oxidative
697 stress conditions. *J Mol Biol* 427(7):1549-1563.
698 30. Winter J, Ilbert M, Graf PC, Ozcelik D, & Jakob U (2008) Bleach activates a
699 redox-regulated chaperone by oxidative protein unfolding. *Cell* 135(4):691-701.
700 31. Yoo NG*, et al.* (2018) Polyphosphate Stabilizes Protein Unfolding Intermediates
701 as Soluble Amyloid-like Oligomers. *J Mol Biol* 430(21):4195-4208.
702 32. Gray MJ & Jakob U (2015) Oxidative stress protection by polyphosphate--new
703 roles for an old player. *Curr Opin Microbiol* 24:1-6.
704 33. Gennaris A*, et al.* (2015) Repairing oxidized proteins in the bacterial envelope
705 using respiratory chain electrons. *Nature* 528(7582):409-412.
706 34. Goemans CV, Vertommen D, Agrebi R, & Collet JF (2018) CnoX Is a
707 Chaperedoxin: A Holdase that Protects Its Substrates from Irreversible Oxidation.
708 *Mol Cell* 70(4):614-627 e617.
709 35. Wang S*, et al.* (2009) Transcriptomic response of Escherichia coli O157:H7 to
710 oxidative stress. *Appl Environ Microbiol* 75(19):6110-6123.

711 36. Basu Thakur P*, et al.* (2019) Complex Responses to Hydrogen Peroxide and
712 Hypochlorous Acid by the Probiotic Bacterium Lactobacillus reuteri. *mSystems*
713 4(5).
714 37. Letunic I & Bork P (2016) Interactive tree of life (iTOL) v3: an online tool for the
715 display and annotation of phylogenetic and other trees. *Nucleic Acids Res*
716 44(W1):W242-245.
717 38. Grozdanov L*, et al.* (2004) Analysis of the genome structure of the
718 nonpathogenic probiotic Escherichia coli strain Nissle 1917. *J Bacteriol*
719 186(16):5432-5441.
720 39. Wassenaar TM (2016) Insights from 100 Years of Research with Probiotic E.
721 Coli. *Eur J Microbiol Immunol (Bp)* 6(3):147-161.
722 40. Chen X*, et al.* (2016) Synthesis of a highly HOCl-selective fluorescent probe and
723 its use for imaging HOCl in cells and organisms. *Nat Protoc* 11(7):1219-1228.
724 41. Macheroux P, Kappes B, & Ealick SE (2011) Flavogenomics--a genomic and
725 structural view of flavin-dependent proteins. *FEBS J* 278(15):2625-2634.
726 42. Lian P*, et al.* (2014) X-ray structure of a Hg2+ complex of mercuric reductase
727 (MerA) and quantum mechanical/molecular mechanical study of Hg2+ transfer
728 between the C-terminal and buried catalytic site cysteine pairs. *Biochemistry*
729 53(46):7211-7222.
730 43. Neidhardt FC, Bloch PL, & Smith DF (1974) Culture medium for enterobacteria. *J*
731 *Bacteriol* 119(3):736-747.
732 44. Hodgkinson V & Petris MJ (2012) Copper homeostasis at the host-pathogen
733 interface. *J Biol Chem* 287(17):13549-13555.

734 45. Ladomersky E & Petris MJ (2015) Copper tolerance and virulence in bacteria.
735 *Metallomics* 7(6):957-964.
736 46. Rensing C & Grass G (2003) Escherichia coli mechanisms of copper
737 homeostasis in a changing environment. *FEMS Microbiol Rev* 27(2-3):197-213.
738 47. Petersen C & Moller LB (2000) Control of copper homeostasis in Escherichia coli
739 by a P-type ATPase, CopA, and a MerR-like transcriptional activator, CopR.
740 *Gene* 261(2):289-298.
741 48. Edward T. Gray RWT, Dale W. Margerum (1977) Kinetics and mechanisms of
742 the copper-catalyzed decomposition of hypochlorite and hypobromite. Properties
743 of a dimeric copper(III) hydroxide intermediate. *Inorg. Chem.* 16(12):3047–3055.
744 49. Liu C, von Gunten U, & Croue JP (2012) Enhanced bromate formation during
745 chlorination of bromide-containing waters in the presence of CuO: catalytic
746 disproportionation of hypobromous acid. *Environ Sci Technol* 46(20):11054-
747 11061.
748 50. Church JA (1994) Kinetics of the Uncatalyzed and Cu(II) -Catalyzed
749 Decomposition of Sodium Hypochlorite. *Ind. Eng. Chem. Res.* 33(2):239-245.
750 51. Lister MW (1956) Decomposition of Sodium Hypochlorite: The Uncatalyzed
751 Reaction. *Canadian Journal of Chemistry* 34:465-478.
752 52. Pham AN, Xing G, Miller CJ, & Waite TD (2013) Fenton-like copper redox
753 chemistry revisited: Hydrogen peroxide and superoxide mediation of copper-
754 catalyzed oxidant production. *Journal of Catalysis* 301:54-64.

755 53. Lisa K. Folkes LPC, 1 and Peter Wardman (1995) Kinetics and Mechanisms of
756 Hypochlorous Acid Reactions. *ARCHIVES OF BIOCHEMISTRY AND*
757 *BIOPHYSICS* 323(1):120-126.
758 54. Conocchioli TJ, Jr. EJH, & Sutin N (1965) The Formation of Iron(IV) in the
759 Oxidation of Iron(II). *J. Am. Chem. Soc. 87* 87(4):926 – 927.
760 55. Hao OJ, Davis AP, & Chang PH (1991) Kinetics of Manganese(II) Oxidation with
761 Chlorine. *Journal of Environmental Engineering* 117(3).
762 56. Allard S, Fouche L, Dick J, Heitz A, & von Gunten U (2013) Oxidation of
763 manganese(II) during chlorination: role of bromide. *Environ Sci Technol*
764 47(15):8716-8723.
765 57. Holmgren A (1976) Hydrogen donor system for Escherichia coli ribonucleoside-
766 diphosphate reductase dependent upon glutathione. *Proc Natl Acad Sci U S A*
767 73(7):2275-2279.
768 58. Yang X & Ma K (2010) Characterization of a thioredoxin-thioredoxin reductase
769 system from the hyperthermophilic bacterium Thermotoga maritima. *J Bacteriol*
770 192(5):1370-1376.
771 59. Rinderle SJ, Booth JE, & Williams JW (1983) Mercuric reductase from R-plasmid
772 NR1: characterization and mechanistic study. *Biochemistry* 22(4):869-876.
773 60. Miller SM, Ballou DP, Massey V, Williams CH, Jr., & Walsh CT (1986) Two-
774 electron reduced mercuric reductase binds Hg(II) to the active site dithiol but
775 does not catalyze Hg(II) reduction. *J Biol Chem* 261(18):8081-8084.
776 61. Sutton HC & Winterbourn CC (1989) On the participation of higher oxidation
777 states of iron and copper in Fenton reactions. *Free Radic Biol Med* 6(1):53-60.

778 62. Gunther MR, Hanna PM, Mason RP, & Cohen MS (1995) Hydroxyl radical
779 formation from cuprous ion and hydrogen peroxide: a spin-trapping study. *Arch*
780 *Biochem Biophys* 316(1):515-522.
781 63. Johnson DK*, et al.* (2015) Stabilization of Cu(I) for binding and calorimetric
782 measurements in aqueous solution. *Dalton Trans* 44(37):16494-16505.
783 64. Morgenstern S, Flor R, Kessler G, & Klein B (1966) The automated determination
784 of NAD-coupled enzymes. II. Serum lactate dehydrogenase. *Clin Chem*
785 12(5):274-281.
786 65. Oikawa S & Kawanishi S (1996) Site-specific DNA damage induced by NADH in
787 the presence of copper(II): role of active oxygen species. *Biochemistry*
788 35(14):4584-4590.
789 66. Mealman TD, Blackburn NJ, & McEvoy MM (2012) Metal export by CusCFBA,
790 the periplasmic Cu(I)/Ag(I) transport system of Escherichia coli. *Curr Top Membr*
791 69:163-196.
792 67. Su CC, Long F, & Yu EW (2011) The Cus efflux system removes toxic ions via a
793 methionine shuttle. *Protein Sci* 20(1):6-18.
794 68. Mateus A*, et al.* (2018) Thermal proteome profiling in bacteria: probing protein
795 state in vivo. *Mol Syst Biol* 14(7):e8242.
796 69. Samanovic MI, Ding C, Thiele DJ, & Darwin KH (2012) Copper in microbial
797 pathogenesis: meddling with the metal. *Cell Host Microbe* 11(2):106-115.
798 70. Letelier ME, Sanchez-Jofre S, Peredo-Silva L, Cortes-Troncoso J, & Aracena-
799 Parks P (2010) Mechanisms underlying iron and copper ions toxicity in biological

800 systems: Pro-oxidant activity and protein-binding effects. *Chem Biol Interact*
801 188(1):220-227.
802 71. Macomber L, Rensing C, & Imlay JA (2007) Intracellular copper does not
803 catalyze the formation of oxidative DNA damage in Escherichia coli. *J Bacteriol*
804 189(5):1616-1626.
805 72. Beveridge SJ, Garrett IR, Whitehouse MW, Vernon-Roberts B, & Brooks PM
806 (1985) Biodistribution of 64Cu in inflamed rats following administration of two
807 anti-inflammatory copper complexes. *Agents Actions* 17(1):104-111.
808 73. Achard ME*, et al.* (2012) Copper redistribution in murine macrophages in
809 response to Salmonella infection. *Biochem J* 444(1):51-57.
810 74. Casciaro M*, et al.* (2017) Chlorinative stress in age-related diseases: a literature
811 review. *Immun Ageing* 14:21.
812 75. Dalle-Donne I, Rossi R, Colombo R, Giustarini D, & Milzani A (2006) Biomarkers
813 of oxidative damage in human disease. *Clin Chem* 52(4):601-623.
814 76. Klebanoff SJ (2005) Myeloperoxidase: friend and foe. *J Leukoc Biol* 77(5):598-
815 625.
816 77. Franceschi C & Campisi J (2014) Chronic inflammation (inflammaging) and its
817 potential contribution to age-associated diseases. *J Gerontol A Biol Sci Med Sci*
818 69 Suppl 1:S4-9.
819 78. Djoko KY & McEwan AG (2013) Antimicrobial action of copper is amplified via
820 inhibition of heme biosynthesis. *ACS Chem Biol* 8(10):2217-2223.
821 79. Rivera-Chavez F & Baumler AJ (2015) The Pyromaniac Inside You: Salmonella
822 Metabolism in the Host Gut. *Annu Rev Microbiol* 69:31-48.

823 80. Shin NR, Whon TW, & Bae JW (2015) Proteobacteria: microbial signature of
824 dysbiosis in gut microbiota. *Trends Biotechnol* 33(9):496-503.
825 81. Datsenko KA & Wanner BL (2000) One-step inactivation of chromosomal genes
826 in Escherichia coli K-12 using PCR products. *Proc Natl Acad Sci U S A*
827 97(12):6640-6645.
828 82. J S, EF F, & T M (1989) *Molecular Cloning: A Laboratory Manual* (Cold Spring
829 Harbor Laboratory Press, Cold Spring Harbor, NY) 2nd Ed.
830 83. Edgar R, Domrachev M, & Lash AE (2002) Gene Expression Omnibus: NCBI
831 gene expression and hybridization array data repository. *Nucleic Acids Res*
832 30(1):207-210.
833

834 SUPPLEMENTAL FIGURES

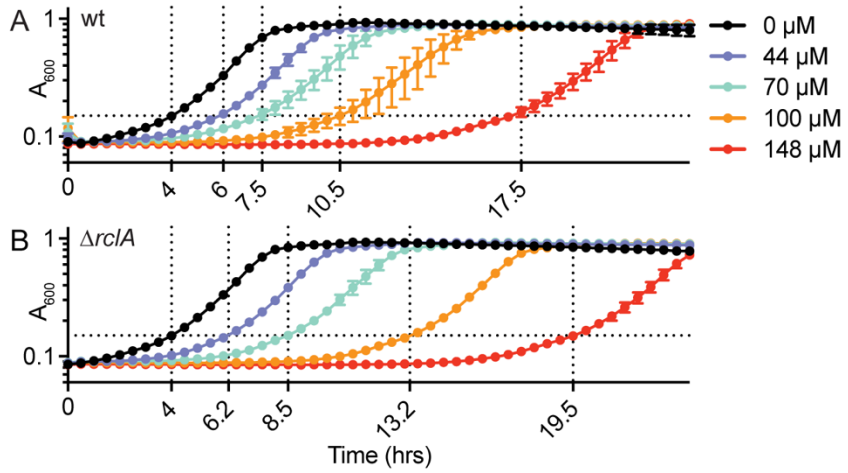

835

836 **Supplemental Figure 1: Growth curve method to determine HOCl sensitivity by**
837 **measuring lag-phase extension.** Overnight cultures of (A) MG1655 wild-type and (B)
838 MJG0046 (Δ*rclA*) were normalized to A_{600} = 0.8 in MOPS minimal media and diluted to
839 A_{600} = 0.08 in MOPS ± HOCl at the indicated concentrations. Cultures were incubated

840 with shaking at 37 °C in a Tecan Infinite M1000 plate reader with A_{600} being measured
841 every hour for 24 hours (n = 3, ± SD). Sensitivity was assessed by comparing lag phase
842 extensions (difference in hours to reach A_{600} ≥ 0.15 from no HOCl control; vertical
843 dotted lines) for each HOCl concentration.
844

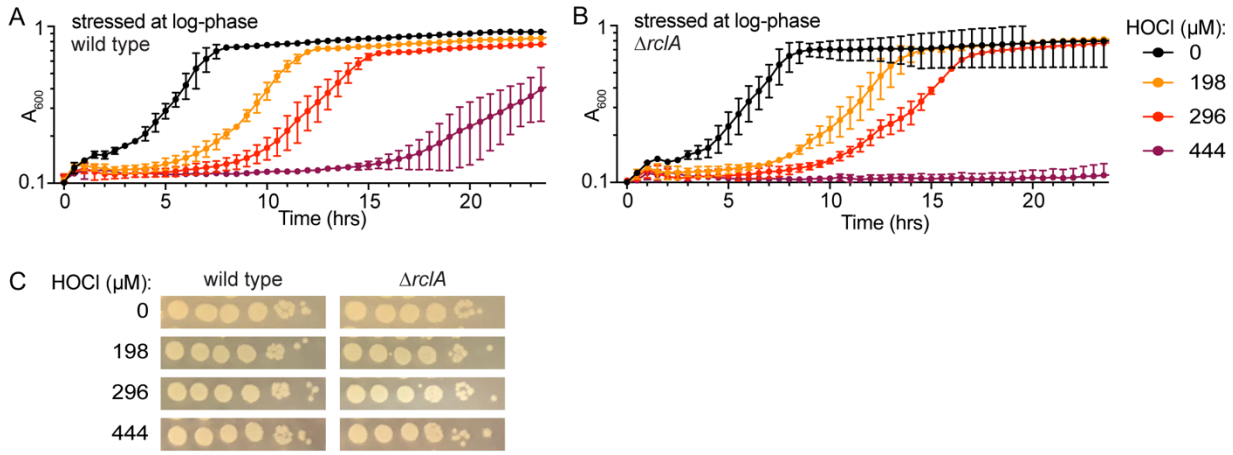

845

846 **Supplemental Figure 2: Lag phase extension of HOCl-treated cells in logarithmic**
847 **growth phase.** HOCl growth curves were performed as in Supplemental Figure 1 but
848 on log-phase cultures of each strain. To prepare the log-phase cultures, saturated
849 overnight cultures were subcultured in MOPS glucose and grown up at 37 °C with
850 shaking at 200 rpm until A_{600} = 0.5. *E. coli* lacking *rclA* (B) had increased lag-phase
851 extensions (LPE) relative to wild type (A) at all the tested HOCl concentrations. The
852 observed growth delays of the strains in the presence of HOCl did not correspond with
853 killing, as determined by viability spot plates (C, pictures representative of 3 biological
854 replicates). Viability spot plates were prepared by collecting 5 μL aliquots from each well
855 used for growth curves 10 minutes after adding MOPS ± HOCl to the OD-normalized

856 cells. Serial dilutions in PBS of the aliquots were performed and 5 µL of the dilutions

857 were spotted on LB plates and grown overnight at 37 °C.

858

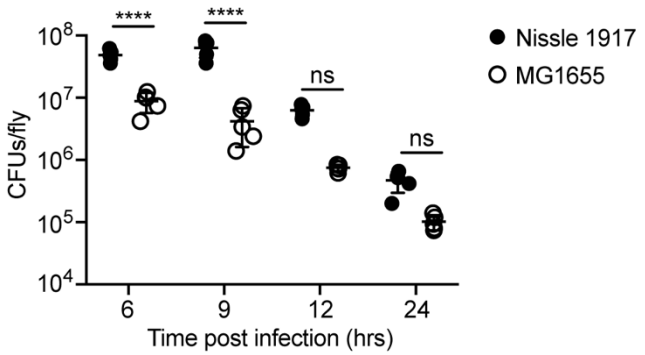

859

860 **Supplemental Figure 3: EcN colonizes Canton^S *D. melanogaster* to a greater**

861 **extent than MG1655.** Flies were fed either *E. coli* MG1655 or EcN and bacterial loads

862 were measured (n = 5, ± SD). Statistical analysis was performed using a two-way

863 ANOVA with Tukey's multiple comparisons test (**** = P < 0.0001, ns = not significant).

864

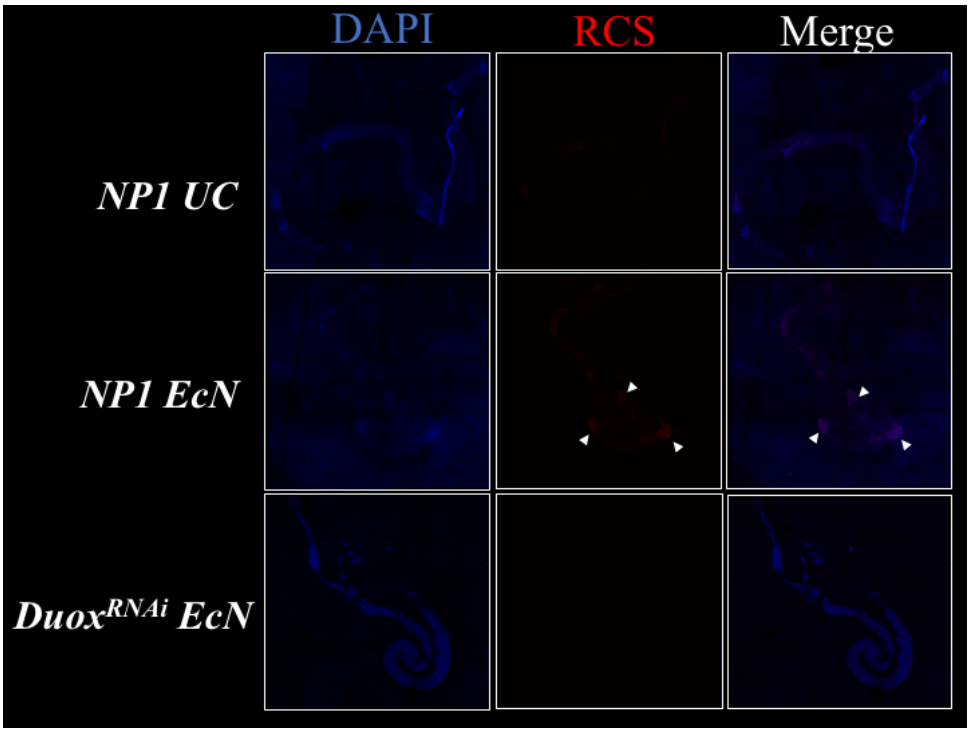

865
866
867 **Supplemental Figure 4: Host-produced HOCl production is silenced by Duox**
868 **RNAi.** *Canton-S* female flies were starved for 2 hours at 29˚C. They were then
869 administered a 1:1 mixture of either *E. coli* Nissle (OD_{600}=200) or LB and 100 μM R19-S
870 prepared in 5% sucrose. After 30 minutes of feeding, all treatments were switched to
871 sucrose/R19-S mixture. 90 minutes after the initial infection, guts were dissected in PBS
872 and fixed in 4% formaldehyde for 50 minutes. Guts were mounted in Vectashield/DAPI
873 and visualized on a Leica SP8 confocal microscope with a red emission range of 530-
874 603.
875

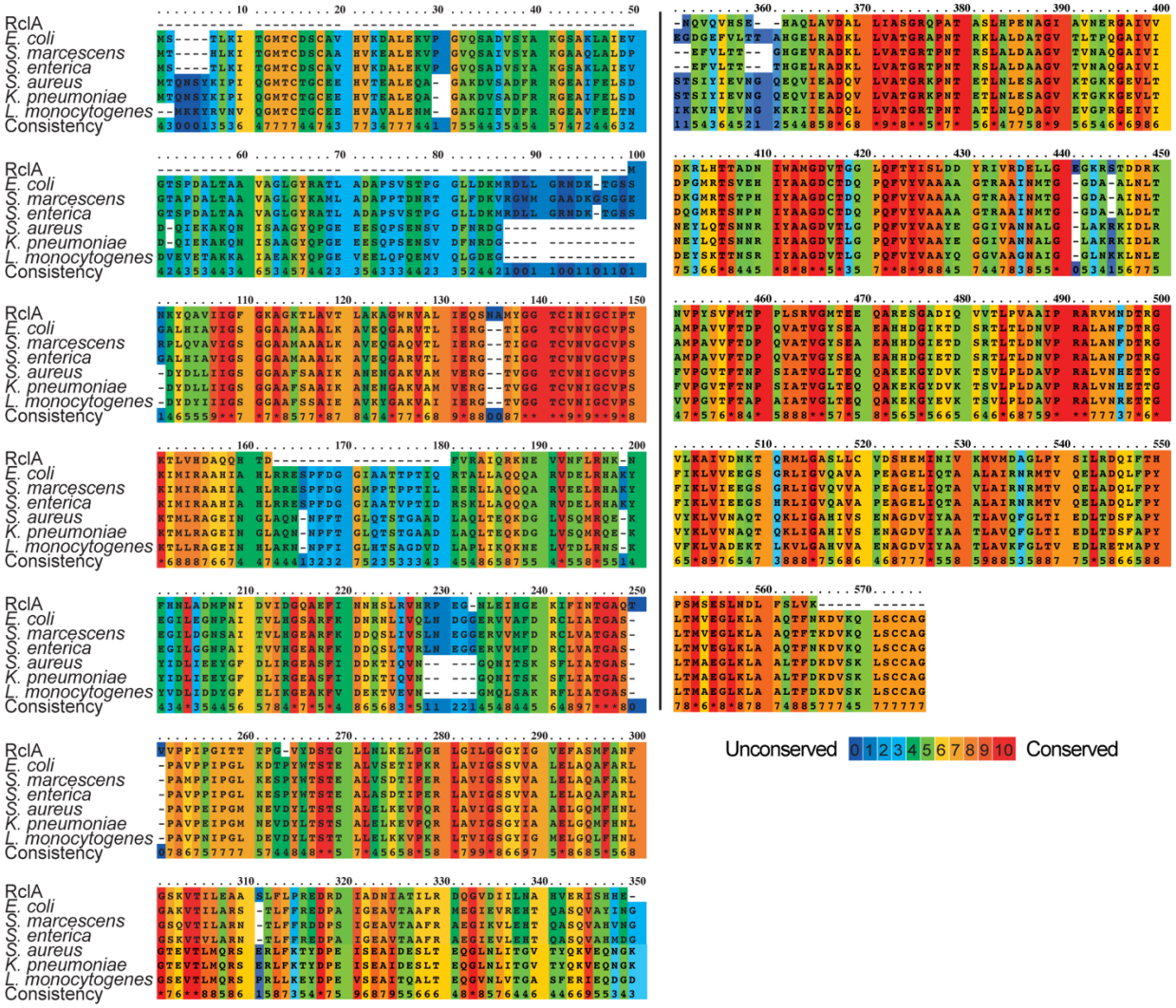

Supplemental Figure 5: Alignment of full length RclA with MerA sequences from representative bacterial species. Alignment of *E. coli* RclA (ADC80840.1) and MerA amino acid sequences from seven species (*Escherichia coli*, ADC80840.1; *Staphylococcus aureus*, AKA87329.1; *Salmonella enterica*, ABQ57371.1; *Listeria monocytogenes*, PDA94520.1; *Klebsiella pneumoniae*, ABY75610.1; *Serratia marcescens*, ADM52740.1). Alignment, conservation scoring, and graphic were made using PRALINE.

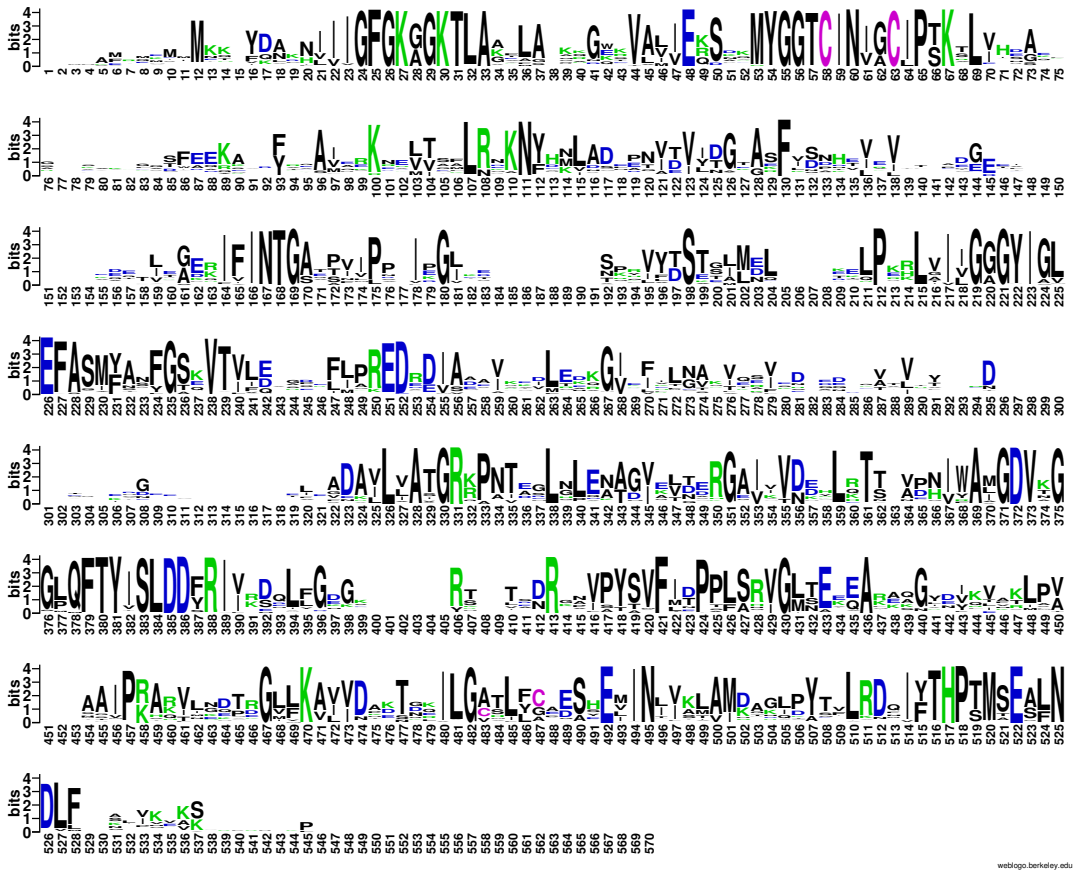

Supplemental Figure 6: Amino acid conservation in RclA sequences from 284 species. Alignment of RclA sequences made using MUSCLE (BLAST e value < $1x10^{-90}$ in 284 species) and graphic made using Weblogo (weblogo.berkeley.edu/logo.cgi). Sequences are from the species represented in Figure 1 and listed in Supplemental Data Table 1.

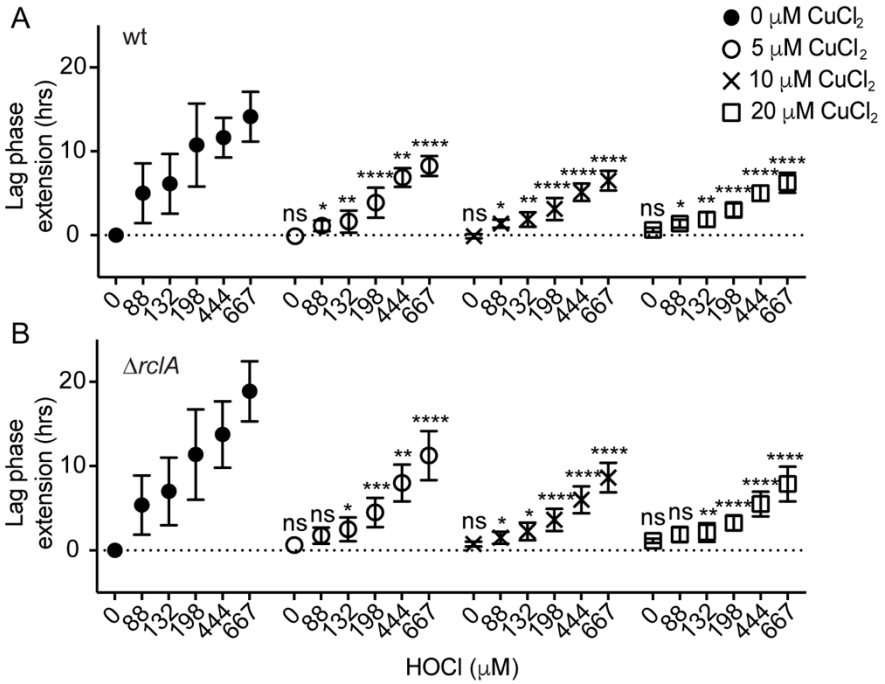

890

891 **Supplemental Figure 7: Extracellular $CuCl_2$ reduces LPE for both wild-type and**
892 **Δ*rclA* *E. coli* grown in the presence of HOCl.** LPE determination for wild-type (A) and
893 Δ*rclA* (B) strains grown in the presence of the indicated HOCl and extracellular $CuCl_2$
894 conditions. Growth curves were performed as described in Supplemental Figure 1 but
895 with supplementing the MOPS glucose with the indicated $CuCl_2$ concentrations. HOCl
896 and $CuCl_2$ were mixed in MOPS minimal media prior to diluting cells A_{600}-normalized to
897 0.08 into each media type. LPEs were calculated by determining the difference in time
898 (hrs) to reach $A_{600} > 0.15$ for each condition relative to no stress controls. Sensitivity
899 was assessed within strains by comparing LPEs for each HOCl/$CuCl_2$ concentration (n
900 = 4, ± SD) at each HOCl concentration (two-way ANOVA for each strain with Dunnett's
901 multiple comparison using the no $CuCl_2$ control for each HOCl concentration,
902 respectively; **** = P < 0.0001, *** = P < 0.001, ** = P < 0.01, * = P < 0.05, ns = not
903 significant).

904

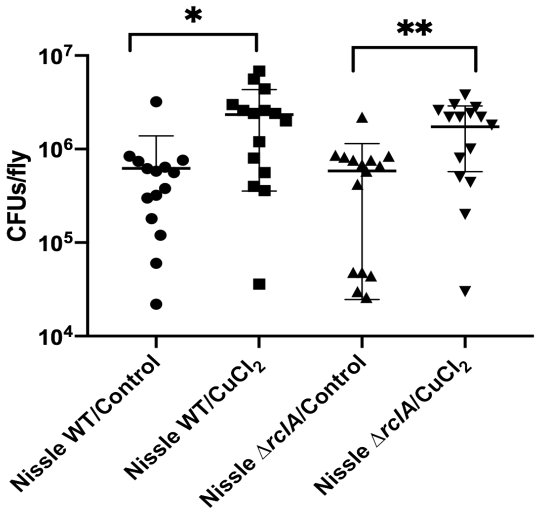

905

906 **Supplemental Figure 8: EcN colonization is improved when flies are fed copper.**

907 *D. melanogaster* Canton^S females fed for 24 hours on a mixture containing sucrose and

908 1mM $CuCl_2$ (or sterile water), which was applied to fly food on a paper disk. Flies were

909 then transferred to new food tubes containing sucrose and either *E. coli* Nissle wild-type

910 (WT) or *E. coli* Nissle Δ*rclA*. Individuals were collected, surface sterilized, homogenized,

911 and plated on LB agar at various time points to determine bacterial load (CFUs/fly).

912 Statistical analysis was performed with GraphPad Prism using a multiple t test with

913 Sidak-Bonferroni correction for multiple comparisons. (N=3, n=60).

914

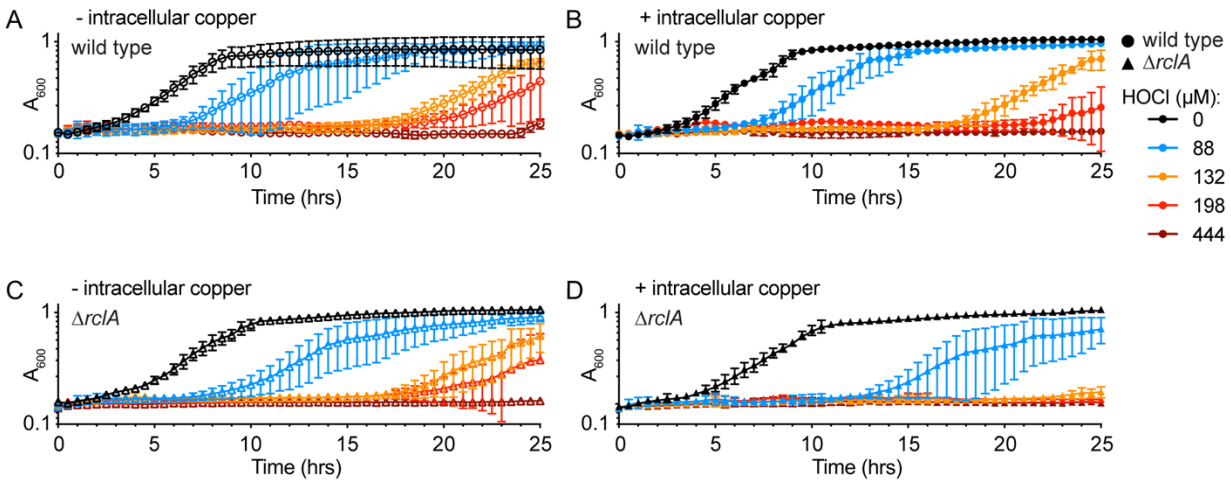

915

916 **Supplemental Figure 9: Absence of intracellular copper reduces HOCl sensitivity**

917 **of *E. coli* lacking *rclA*.** Wild type (A and B) and Δ*rclA* (C and D) *E. coli* were grown up

918 overnight in MOPS glucose with (B and D) and without copper (A and C). HOCl growth

919 curves were performed as described in Figure 6.

920

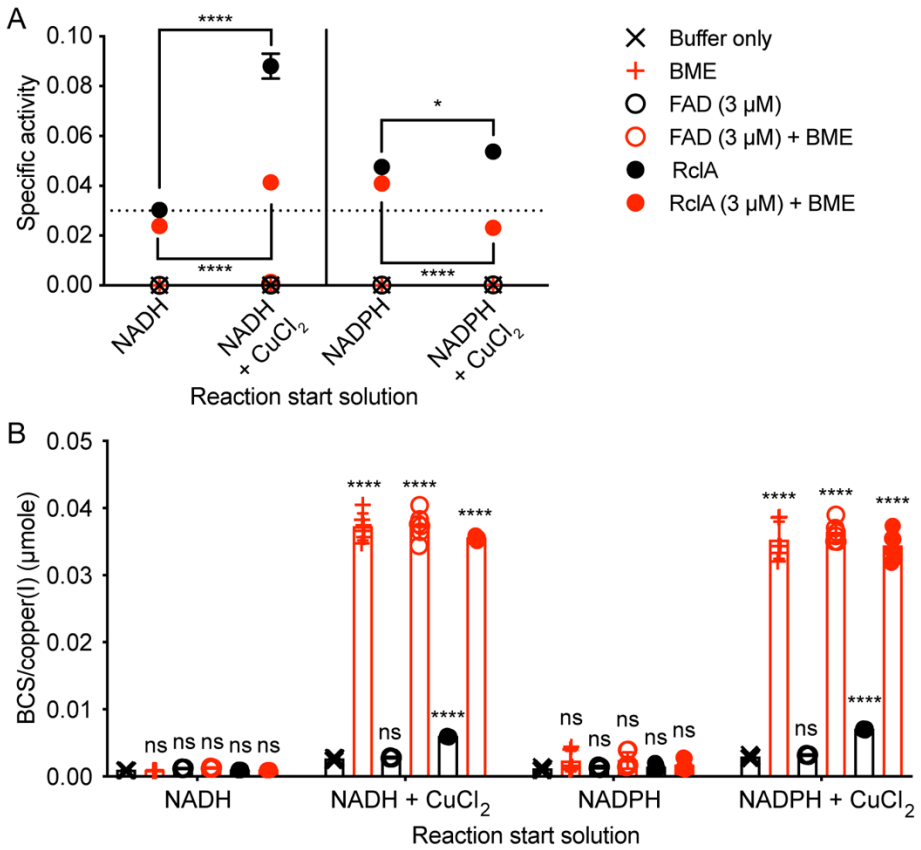

Supplemental Figure 10: Adding BME to the start solutions of RclA reactions does not increase SA and causes Cu(I) accumulation. RclA reactions performed as in Figure 7 but with the addition of 1 mM BME for indicated samples (n = 6, ± SD). SA (A) and BCS/Cu(I) concentration determined as in Figure 7. Differences in SA in the presence of each metal were analyzed using a two-way ANOVA with Dunnet's multiple comparison test using the buffer only sample as the control for each start solution (****= P < 0.0001).

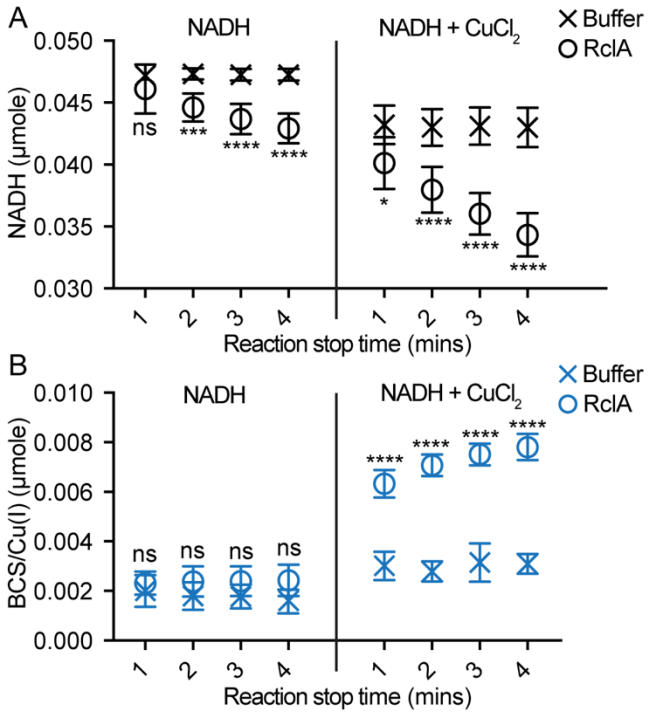

Supplemental Figure 11: Changes in NADH and copper (I) concentrations over time during the RclA reaction. NADH oxidation (A) and BCS/Cu(I) complex formation (B) were measured over time spectrophotometrically with and without RclA. Reactions were started by adding 100 µL of NADH (200 µM final) or NADH and $CuCl_2$ (both 200 µM final) to 100 µL of RclA (3 µM final) at 37 ˚C using the injector system of a Tecan Infinite M1000 plate reader. All reactions were carried out in 20 mM HEPES, 100 mM NaCl, pH 7. NADH absorbance at 340 nm was measured each minute for the indicated reaction times. Each reaction was then stopped at the indicated times with 10 µL of a BCS (400 µM final) and EDTA (1 mM final) solution using the injector system of the plate reader (n = 6 for each reaction type, ± SD). The stopped reactions were incubated at 37 ºC for 5 minutes with the absorbance of BCS/Cu(I) complex being measured at 483 nm each minute to ensure saturation of BCS. Reported BCS/Cu (I) values were calculated using the average of the total absorbance measurements over the five-

945 minute incubation because the values were stable over that time. Differences in the
946 amount of NADH or BCS/Cu(I) complex between the buffer only and RclA reactions
947 were analyzed using a 2-way ANOVA with Sidak's multiple comparison test (**** = P <
948 0.0001, *** = P < 0.001, * = P < 0.05, ns = not significant).
949

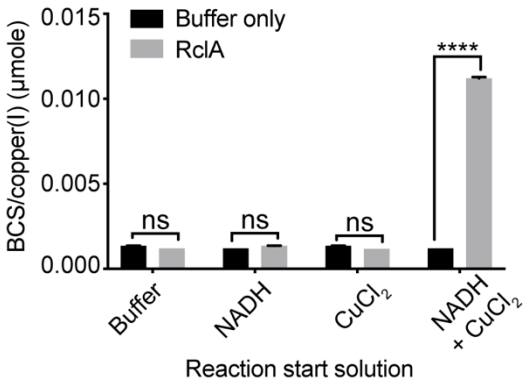

950

951 **Supplemental Figure 12: The copper reductase activity of RclA is maintained**
952 **under anerobic conditions.** BCS/Cu(I) complex concentrations were determined as in
953 Figure 7 but all reactions were performed in an anaerobic chamber (n = 6, ± SD).
954 Differences in the amount of BCS/Cu(I) complex between the buffer only and RclA (3
955 µM) reactions were analyzed using a two-way ANOVA with Tukey's multiple comparison
956 test (****= P < 0.0001, ns = not significant).
957

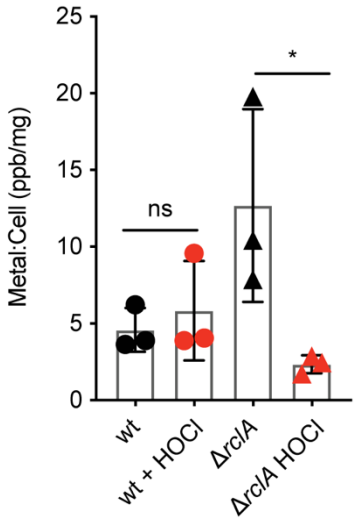

958

959 **Supplemental Figure 13: Intracellular copper concentrations do not change after**

960 **HOCl stress in wildtype *E. coli*.** Intracellular copper before and after HOCl stress (30

961 min at 400 μM) of wild-type (wt) and Δ*rclA* mutant strains was determined using ICP-

962 MS. Differences between intracellular copper analyzed using a two-way ANOVA with

963 Tukey's multiple comparison test (* = P < 0.05, ns = not significant).

964

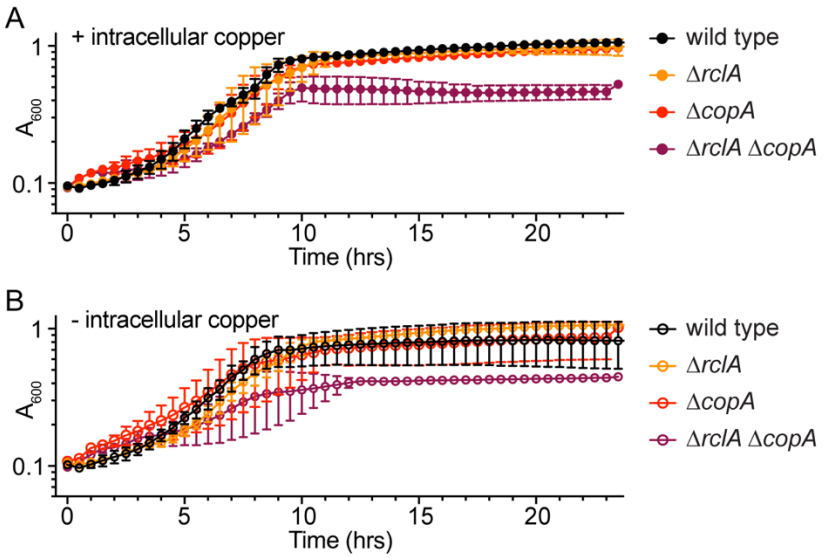

965

966 **Supplemental Figure 14: *rclA copA* mutants have a growth defect in copper-free**
967 **media.** A double mutant of *rclA* and *copA* has a growth defect when grown in copper-
968 free MOPS when subcultured from overnight cultures grown either with (A) or without
969 copper (B). HOCl growth curves on cells with and without intracellular copper were
970 performed as described in Figure 6 with copper-free MOPS glucose (n = 3).
971

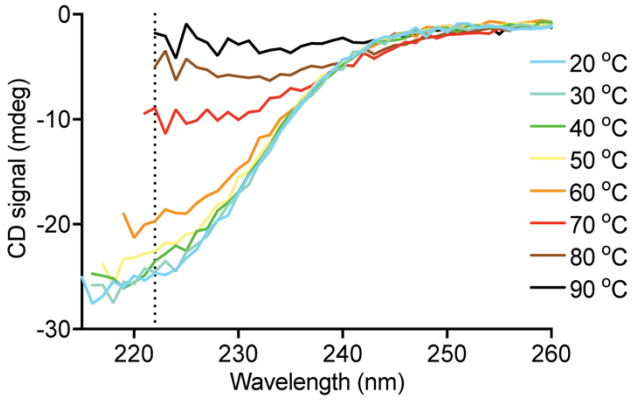

972
973 **Supplemental Figure 15: The melting temperature (T_m) of RclA is approximately**
974 **10 °C higher than the average T_m of the *E. coli* proteome.** (A) CD spectra of RclA
975 measured at indicated temperatures; 222 nm is indicated with a vertical dashed line.
976

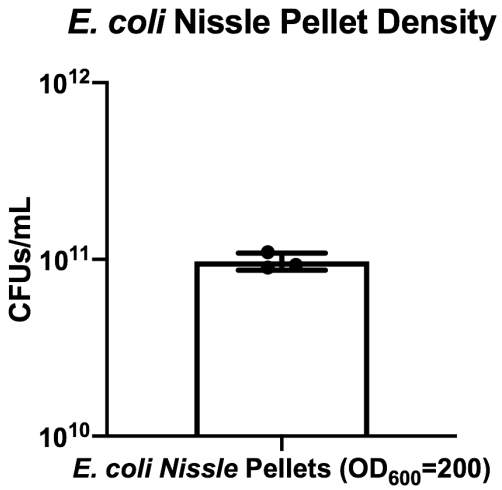

977
978

979 **Supplemental Figure 16: *E. coli Nissle* pellets contain consistent bacterial**

980 **density.** Three independent *E. coli Nissle* cultures were grown in 30 ml of LB at 37˚C

981 with shaking for 20 hours. Cultures were pelleted by centrifugation at 3,428 x g.

982 Resulting pellets were adjusted to an OD_{600} of 200. Dilutions were plated to determine

983 CFUs/ml.